

การประยุกต์การตรวจวัดทางเคมีไฟฟ้าสำหรับระบบไมโครฟลูอิดิกส์ที่เป็นหยด
ของเหลวขนาดเล็ก

An Application of electrochemical detection for droplet-based microfluidics

นายอัคพล เสื่องาม

เลขประจำตัว

5333141023

เคมี



ภาควิชาเคมี
คณะวิทยาศาสตร์
จุฬาลงกรณ์มหาวิทยาลัย

การประยุกต์การตรวจวัดทางเคมีไฟฟ้าสำหรับระบบไมโครฟลูอิดิกส์ที่เป็นหยด
ของเหลวขนาดเล็ก

An Application of electrochemical detection for droplet-based
microfluidics



โดย

นายอัคพล เสืองาม

รายงานนี้เป็นส่วนหนึ่งของการศึกษาตามหลักสูตร

ปริญญาวิทยาศาสตรบัณฑิต

ภาควิชาเคมี คณะวิทยาศาสตร์

จุฬาลงกรณ์มหาวิทยาลัย

ปีการศึกษา 2556

เรื่อง การประยุกต์การตรวจวัดทางเคมีไฟฟ้าสำหรับระบบไมโครฟลูอิดิกส์ที่เป็นหยดของเหลว
ขนาดเล็ก

โดย นายอัศพล เสืองาม

ได้รับอนุมัติให้เป็นส่วนหนึ่งของการศึกษา

ตามหลักสูตร ปริญญาวิทยาศาสตรบัณฑิต ภาควิชาเคมี

คณะวิทยาศาสตร์ จุฬาลงกรณ์มหาวิทยาลัย

คณะกรรมการสอบโครงการ

..... ประธานกรรมการ

(ศาสตราจารย์ ดร.อรวรรณ ชัยลภากุล)

..... อาจารย์ที่ปรึกษา

(อาจารย์ ดร.มนพิชา ศรีสะอาด)

..... กรรมการ

(อาจารย์ ดร.คณศ วงษ์ระวี)

รายงานฉบับนี้ได้รับความเห็นชอบและอนุมัติโดย หัวหน้าภาควิชาเคมี

.....

(รองศาสตราจารย์ ดร.วุฒิชัย พาราสุข)

หัวหน้าภาควิชาเคมี

วัน.....เดือน.....พ.ศ.

ชื่อโครงการ การประยุกต์ระบบตรวจวัดทางเคมีไฟฟ้าสำหรับระบบไมโครฟลูอิดิกส์ที่เป็นหยด
ของเหลวขนาดเล็ก

ชื่อนิสิตในโครงการ นายอัคพล เสืองาม เลขประจำตัว 5333141023

อาจารย์ที่ปรึกษา อ.ดร.มนพิชา ศรีสะอาด

ภาควิชา เคมี คณะวิทยาศาสตร์ จุฬาลงกรณ์มหาวิทยาลัย ปีการศึกษา 2556

บทคัดย่อ

ในงานนี้ได้เสนอการประยุกต์ระบบไมโครฟลูอิดิกส์ที่เป็นหยดของเหลวขนาดเล็ก ควบคู่กับระบบตรวจวัดทางเคมีไฟฟ้าโดยใช้โครโมแอมเปโรเมตรีกับขั้วไฟฟ้าคาร์บอนบนไมโครชิป สำหรับการตรวจวัดโดปามีนและกรดแอสคอร์บิก หยดของเหลวขนาดเล็กถูกสร้างขึ้นโดยใช้อัตราการไหลของน้ำมันที่ 1.8 ไมโครลิตรต่อนาที่ ในขณะที่ใช้อัตราการไหล 0.8 ไมโครลิตรต่อนาที่สำหรับเฟสที่เป็นน้ำ ซึ่งให้ค่าสัดส่วนของน้ำเท่ากับ 0.31 ค่าศักย์ไฟฟ้าที่เหมาะสมสำหรับการตรวจวัดด้วยระบบโครโมแอมเปโรเมตรีคือ 150 มิลลิโวลต์ การวิเคราะห์ที่มีความเที่ยงสูงของโดปามีนและกรดแอสคอร์บิก ให้ค่าความคลาดเคลื่อนสัมพัทธ์ต่ำกว่า 5 เปอร์เซ็นต์สำหรับทั้งการตรวจวัดระหว่างวันและภายในหนึ่งวัน ขีดจำกัดของการตรวจวัดและค่าที่ต่ำที่สุดที่สามารถการหาปริมาณวิเคราะห์ได้เท่ากับ 20 ไมโครโมลาร์และ 70 ไมโครโมลาร์ สำหรับโดปามีน และ 41 และ 137 ไมโครโมลาร์สำหรับกรดแอสคอร์บิก ช่วงความเป็นเส้นตรงของวิธีนี้อยู่ในช่วง 0.02 ถึง 3.0 มิลลิโมลาร์ สำหรับโดปามีน และ 0.04 ถึง 3.0 มิลลิโมลาร์สำหรับกรดแอสคอร์บิก ระบบนี้ได้ถูกประยุกต์สำหรับการหาปริมาณโดปามีนและกรดแอสคอร์บิกในยาสำหรับฉีด กราฟมาตรฐานของโดปามีนและกรดแอสคอร์บิกสำหรับการหาปริมาณวิเคราะห์ ให้ค่าความเป็นเส้นตรงโดยมีค่า R^2 เท่ากับ 0.9970 และ 0.9982 ตามลำดับ เมื่อเทียบกับปริมาณที่ระบุพบว่าความเข้มข้นของโดปามีนและกรดแอสคอร์บิก ที่วัดได้จากระบบนี้แตกต่างกันเพียงเล็กน้อย โดยมีเปอร์เซ็นต์ความผิดพลาดเท่ากับ +1.8 เปอร์เซ็นต์ สำหรับกรดแอสคอร์บิก และเปอร์เซ็นต์ความผิดพลาดอยู่ในช่วง -2.6 ถึง -5.7 เปอร์เซ็นต์ สำหรับโดปามีน ซึ่งแสดงถึงความถูกต้องของวิธีพัฒนาขึ้น

คำสำคัญ: ระบบไมโครฟลูอิดิกส์ที่เป็นหยดของเหลวขนาดเล็ก, การตรวจวัดทางเคมีไฟฟ้า,
โดปามีน, กรดแอสคอร์บิก

Title Applications of electrochemical detection for droplet-based microfluidics

Student name Mr.Akkpol Suea-Ngam ID 5333141023

Advisor Monpichar Srisa-Art, Ph.D.

Department of Chemistry, Faculty of Science, Chulalongkorn University, Academic year 2013

Abstract

Here, an application of droplet-based microfluidics coupled with an electrochemical sensor using chronoamperometry with chip-based carbon paste electrodes (CPEs) for determination of dopamine (DA) and ascorbic acid (AA) was presented. Droplets were generated using an oil flow rate of 1.8 $\mu\text{L}/\text{min}$ whereas a flow rate of 0.8 $\mu\text{L}/\text{min}$ was applied for an aqueous phase, which given water fraction equal to 0.31. An optimum applied potential for chronoamperometric measurements in droplet was found to be 150 mV. Highly reproducible analysis of DA and AA was achieved with relative standard deviations less than 5% for both intraday and inter-day measurements. Limit of detection (LOD) and limit of quantitation (LOQ) were found to be 20 and 70 μM for DA and 41 and 137 μM for AA. The dynamic range of this method was in the ranges of 0.02-3.0 mM for DA and 0.04-3.0 mM for AA. This system was successfully applied to determine the amount of DA and AA in intravenous drugs. Calibration curves of DA and AA for quantitative analysis were obtained with good linearity with R^2 values of 0.9970 and 0.9982, respectively. Compared with the labeled amounts, the measured concentrations of DA and AA obtained from this system were slightly different with the error percentages of +1.8% for AA and in the range of -2.6 to -5.7% for DA, indicating high accuracy of the developed method.

Keywords: Droplet-based microfluidics, Electrochemical sensor, Dopamine, Ascorbic acid

ACKNOWLEDGEMENTS

Firstly, I would like to express my deeply impressed to my advisor, Dr. Monpichar Srisa-Art, for her mercy, kindness, tolerance, exertion, valuable suggestions and critical reading. Also, I am very thankful to Professor Dr.Orawon Chailapakul who always encouraged and gave a support to my work. In addition, I would like to thank to Mr.Poomrat Rattanarat for the help and great suggestion.

Furthermore, I specially thank to all members of Chromatography and separation research unit and Electrochemistry and optical spectroscopy research unit for their useful suggestion. Also, I am thankful to all members of microfluidic research group for their helpfulness. A big patience of my friends for listening to my words is much appreciated.

Finally, I am grateful to be my father's son and very thankful for the rest of the family members. Also, I would like to express all my respect to the lord Buddha and all his discipline for making me a better man.

Akkapol Suea-Ngam

ภาควิชาเคมี
คณะวิทยาศาสตร์
จุฬาลงกรณ์มหาวิทยาลัย

CONTENTS

	PAGE
ABSTRACT (IN THAI)	iii
ABSTRACT (IN ENGLISH)	iv
ACKNOWLEDGEMENTS	v
CONTENTS	vi
LIST OF TABLES	ix
LIST OF FIGURES	x
LIST OF ABBREVIATIONS AND SYMBOLS	xiii
CHAPTER 1 : INTRODUCTION	1
1.1 What is Microfluidics?	1
1.2 Droplet-based Microfluidics	1
1.3 Detection in Droplets	2
1.4 Application of Droplet-based Microfluidics	3
1.5 Literature Review	3
1.6 Scope and Aims of this Work	6
CHAPTER 2 : THEORY	7
2.1 Droplet-based Microfluidics	7
2.1.1 Droplet generation	7
2.1.2 Droplet size	9
2.1.2.1 Water fraction	9
2.1.3 Flow velocity	10
2.1.4 Mixing in droplet	11
2.2 Microchip Fabrication	13
2.3 Electrochemical Detection	14
2.3.1 Cyclic voltammetry	14
2.3.2 Chronoamperometric detection	15
CHAPTER 3 : METHODOLOGY	17
3.1 Chemicals and Equipment	17
3.2 Device Fabrication	18
3.2.1 PDMS mold fabrication	18

3.2.2	PDMS casting	20
3.2.3	Electrode fabrication	22
3.2.4	PDMS microchip assembly	24
3.2.5	Electric wire connection	25
3.3	Preparation of Solution	27
3.3.1	Phosphate buffer saline	27
3.3.2	Standard solutions of dopamine (DA) and ascorbic acid (AA)	27
3.3.3	Sample solutions	28
3.4	Experimental Setup	29
3.4.1	Electrochemical performance	29
3.4.2	Droplet generation	30
3.4.3	Chronoamperometry in microdroplet	31
3.4.3.1	Hydrodynamic voltammogram	31
3.4.3.2	Effect of water fraction (W_f)	32
3.4.3.3	Effect of total flow rate	32
3.5	Method of Validation	33
3.5.1	Calibration curve	33
3.5.2	Linearity	33
3.5.3	Limit of detection (LOD) and limit of quantitation (LOQ)	34
3.5.4	Precision	34
3.6	Sample Measurements	35
CHAPTER 4 : RESULTS AND DISCUSSION		36
4.1	Electrochemical Performance	36
4.1.1	Cyclic voltammogram	36
4.2	Droplets with Electrochemical Detection	39
4.2.1	Hydrodynamic voltammogram	40
4.2.2	Chronoamperometry in droplets	42
4.2.3	Effect of water fraction on chronoamperometric detection	43

4.2.4	Effect of total flow rate on chronoamperometric detection	45
4.3	Method of Validation	47
4.3.1	Calibration curve	47
4.3.2	Limit of detection (LOD) and limit of quantitation (LOQ)	51
4.3.3	Linearity	51
4.3.4	Precision	53
4.4	Real Sample Measurements	55
Chapter 5 : CONCLUSIONS		57
REFERENCES		59
VITA		63



LIST OF TABLES

TABLES		PAGE
3.1	Volumes of stock solutions pipetted to prepare a concentration series of DA and AA.	28
3.2	Volumes of pipetted real samples to prepare DA and AA sample solutions at concentrations of 1.0 and 1.5 mM, respectively.	29
3.3	Flow rates applied to each inlet to study effect of W_f .	32
3.4	Flow rates applied to each inlet to study effect of total flow rate on chronoamperometry in droplet.	33
4.1	Effect of water fraction on chronoamperometric measurements of 1 mM dopamine when using total flow rate of 2.6 $\mu\text{L}/\text{min}$ and a 150 mV applied potential.	43
4.2	Effect of total flow rate on amperometric measurements of 1 mM DA when using $W_f = 0.31$ and 150 mV applied potential.	45
4.3	Inter-day measurements of DA and AA. The experiments were carried out in 3 days ($n = 3$).	53
4.4	Intraday precision of DA and AA measurements. The currents were averaged from 50 droplets ($n = 50$) for each concentration.	55
4.5	The concentrations of DA and AA in real samples which are measured using the droplet system.	56

LIST OF FIGURES

FIGURES		PAGE
1.1	(a) a laminar-flow microfluidic system (b) droplet-based microfluidics. Reproduced from reference 3.	2
1.2	Electrochemical detection in laminar flow-based microfluidics. Reproduced from reference 14.	3
1.3	Electrochemical detection of droplets using amperometry (a) A pattern of microfluidic device (b) droplet generation (c) electrochemical measurements on each droplet. Reproduced from reference 19.	4
1.4	Amperometric detection for a droplet-based microfluidic system. The detection system consists of coupled microelectrodes incorporated with microdevices. Reproduced from reference 21.	5
1.5	A microfluidic device with a narrow microchannel for elongation of droplets. Microband gold microelectrodes were placed across the narrow channel for detection of elongated droplets. Reproduced from reference 23.	6
2.1	Droplet generation in a T-junction microfluidic device. Reproduced from reference 26.	8
2.2	Droplet generation at different water fractions. Reproduced from reference 28.	10
2.3	A model to explain the mixing of two reagents by chaotic advection; Photographs of two layers of the modeling clay being stretched and folded. Reproduced from reference 29.	12
2.4	Comparison of a) laminar flow microfluidics and b) droplet-based microfluidics. The droplet system exploits a winding channel to generate rapidly chaotic mixing. Reproduced from reference 3.	12
2.5	Microchip fabrication (a) a design (using AutoCAD) printed on a film mask (b) making of reservoirs (c) PDMS casting (d) removal of a PDMS replica (e) PDMS bonding to enclose the system. Reproduced from reference 32.	13
2.6	A typical cyclic voltammogram. E_{pc} is cathodic peak potential, i_{pc} is cathodic peak current, E_{pa} is anodic peak potential and i_{pa} is anodic peak current. Reproduced from reference 35.	15
2.7	Hydrodynamic voltammogram plotted using the signal-to-noise ratio as a function of the applied potential of 100 μ M Dithiotheritol injection. Reproduced from reference 25.	16

3.1	Complete SU-8 masters on silicon wafers a) microchannel patterned and b) electrodes patterned master.	19
3.2	Fabrication process of a PDMS master using an SU-8 photoresist.	20
3.3	Summary of a PDMS casting process for microfluidic device fabrication.	21
3.4	PDMS replicas; a) microchannel patterned PDMS and b) electrode patterned PDMS. A red dye was filled into the channel in a) for visualization.	22
3.5	The paste for electrode fabrication and an electrode-patterned PDMS plate.	23
3.6	The electrode paste was filled into the channels on a PDMS plate.	23
3.7	The electrode paste was spread to fill the microchannels.	23
3.8	Removal of excess electrode paste using Scotch Magic Tape™.	24
3.9	The patterned CPEs on a PDMS plate.	24
3.10	Connection of wires to the electrodes.	26
3.11	Silver paste as a connector between the wires and electrodes.	26
3.12	A complete microfluidic device for electrochemical detection.	27
3.13	A microfluidic device for batch measurements. The device has a small well with 2 cm i.d. covering the CPEs.	30
3.14	The experimental set up of a droplet-based microfluidic device with electrochemical detection. The device is placed on microscope stage for visualization.	31
4.1	Voltammograms of 0.1 mM dopamine in 0.1 M PBS (pH 7.4) generated using (a) irreversible oxygen plasma bonding (b) reversible ethanol bonding devices.	37
4.2	Cyclic voltammograms of dopamine and ascorbic acid when generated using the reversible bonding chip.	38
4.3	Chronoamperometric currents of dopamine, ascorbic acid and background electrolyte at different applied potentials. Droplet were generated using total flow rate of 2.6 $\mu\text{L}/\text{min}$ (54 mm/s) and $W_f = 0.31$.	40
4.4	Hydrodynamic voltammograms of dopamine and ascorbic acid. Conditions for droplet generation are shown in Figure 4.3.	41

- 4.5 Chronoamperometric readouts of 35-s window for droplets containing 2 mM DA (a) and AA (b) in 0.1 M PBS pH 7.4. This experiment was carried out using a total flow rate of 2.6 $\mu\text{L}/\text{min}$ (0.016 mm/s) and $W_f = 0.31$. The applied potential was 150 mV. 42
- 4.6 Effect of W_f on amperometric measurements. Droplets were generated using 1 mM DA with total flow rate of 2.6 $\mu\text{L}/\text{min}$ and the applied potential was 150 mV. 44
- 4.7 Effect of total flow rate on amperometric measurements. Droplet were generated using 1 mM DA with $W_f = 0.31$ and 150 mV applied potential. 46
- 4.8 Chronoamperometric signals obtained from a single droplet containing different (a) DA and (b) AA concentrations. Droplets were generated using total flow rate of 2.6 $\mu\text{L}/\text{min}$ and $W_f = 0.31$. The applied potential was 150 mV. 48
- 4.9 Chronoamperograms of (a) DA and (b) AA at different concentrations measured from the droplet system. 49
- 4.10 Calibration curves of (a) DA and (b) AA. Conditions for droplet formation and the applied potential were the same as in Figure 4.8. 50
- 4.11 The linear range of current signals obtained from the droplet system with electrochemical detection when measuring DA (a) and AA (b) at different concentrations. Other conditions for droplet generation and the applied potential are shown in Figure 4.8. 52
- 4.12 Amperometric currents obtained from measurements of 50 droplets containing 0.5, 1.5 and 2.5 mM DA (a) and AA (b). Each concentration was separately measured. Other conditions are shown in Figure 4.8. 54

LIST OF ABBREVIATIONS AND SYMBOLS

AA	Ascorbic acid
BG	Background electrolyte
CPE	Carbon paste electrode
DA	Dopamine
LOC	Lab on a chip
PBS	Phosphate buffer saline
PDMS	Polydimethyl siloxane
PFD	Perfluorodecaline
S/N	Signal to noise ratio
A	Droplet area in microchannel
C_{det}	Determined concentration
$C_{labeled}$	Labeled concentration
F_o	Flow rate of a carrier phase
F_T	Total flow rate
F_w	Flow rate of an aqueous phase
W_f	Water fraction
V	Flow velocity
V_T	Droplet velocity
γ	Surface tension
μ	Viscosity of the fluid
μ TAS	Micro total analysis system
\bar{x}	Averaged current

จุฬาลงกรณ์มหาวิทยาลัย
 คณะวิทยาศาสตร์
 ภาควิชาเคมี

Chapter 1

Introduction

1.1 What's Microfluidics?

Micro-total analysis system (μ TAS) or lab-on-a-chip technology (LOC) is a powerful tool for manipulating the micro systems in analytical and biochemical fields. The concept of LOC is to manage all-in-one systems, such as sample preparation and introduction reaction, separation and detection. Microfluidics is a system that follows the concept of μ TAS. Accordingly, this system manipulates small amounts of fluids, using channels or chambers with dimensions of tens to hundreds of micrometers. Although this system requires very small quantities of samples and reagents, it exhibits high resolution and sensitivity of separation and detection; low cost; short analysis time and small footprints for the analytical devices.¹

1.2 Droplet-based Microfluidics

Due to small dimensions, laminar flow is typically predominant in microfluidic systems. This laminar flow causes two classic problems associated with continuous flow microfluidic systems; mixing is slow and dispersion of solutes along the channel is large. Accordingly, there have been efforts to solve these problems. For example, segmented flow for applications to microfluidics was reported by Quake et al.² to solve the problems associated with analytical applications of microfluidic systems at that time. However, solving the mixing problem was successfully achieved by Song et al.³ using microdroplets generated in normal microfluidic platforms, which is widely known as droplet-based microfluidics. For this system, aqueous droplets are generated in microchannels using two immiscible phase, such as aqueous and oil

solutions. Oil is often used as a carrier phase and an aqueous solution is often used as a dispersed phase. Droplets encapsulate and carry samples along the microchannels with rapid mixing and no dispersion. The generated droplets can be served as small containers for chemical reactions. Figure 1.1 shows a comparison between a traditional laminar-flow microfluidic system and droplet-based microfluidics.

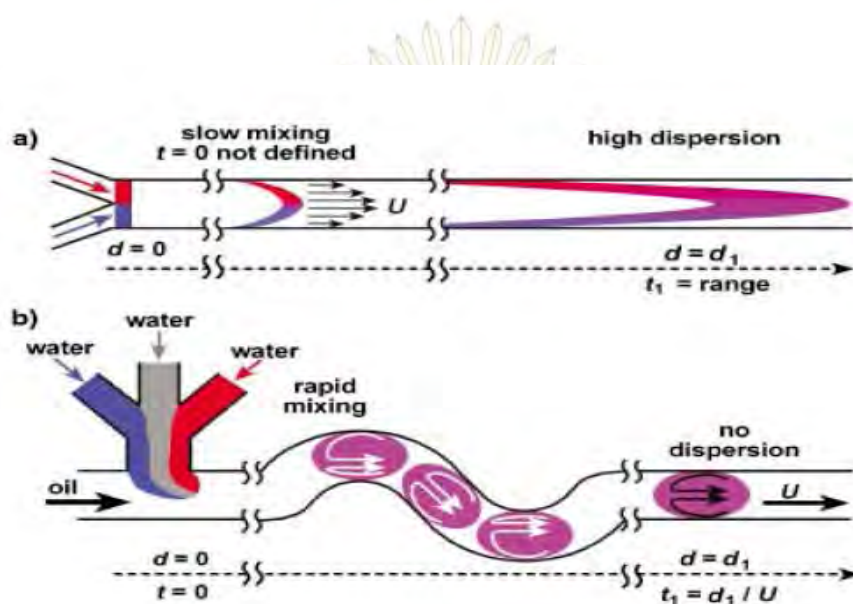


Figure 1.1 (a) a laminar-flow microfluidic system (b) droplet-based microfluidics.

Reproduced from reference 3.

1.3 Detection in Droplets

There are many methods for detection the quantity of analytes in droplet-based microfluidic systems⁴⁻⁵. The well-known methods are fluorescence spectroscopy, Raman spectroscopy, mass spectrometry and electrochemical methods. Optical detection, especially fluorescence detection⁶⁻⁷, is normally favorable for microfluidic systems, because of high precision and accuracy, low limit of detection and suitable connection to microfluidic devices. Even though fluorescence detection has many advantages, this technique requires complicated and large instrumentation and it is expensive. Electrochemical detection, which is cheap and portable, can be an

alternative for detection in microfluidic systems. Therefore, electrochemical detection could be an attractive detector for droplet-based microfluidics.

1.4 **Applications of Droplet-based Microfluidics**

There have been many research groups using droplet-based microfluidics for increasing the ability of their analytical measurements. Droplet-based microfluidics is very useful in many fields, such as synthesis of organic compounds⁸, synthesis of metal nanoparticles⁹, liquid-liquid extraction¹⁰, enzymatic assays¹¹, biological assays¹² and medical applications.¹³

1.5 **Literature Review**

Moehlenbrock et al.¹⁴ reported detection in laminar microfluidic systems using both fluorescence and electrochemical techniques. Amperometry for electrochemical detection was applied for detection of glutathione. The amperometric detection was performed through a metal working microelectrode incorporated into the channel on the left side of the microdevice (Figure 1.2). In this study, researchers found that limit of detection of the electrochemical sensor for detection of glutathione was down to 155 nM with sensitivity as high as fluorescence technique.

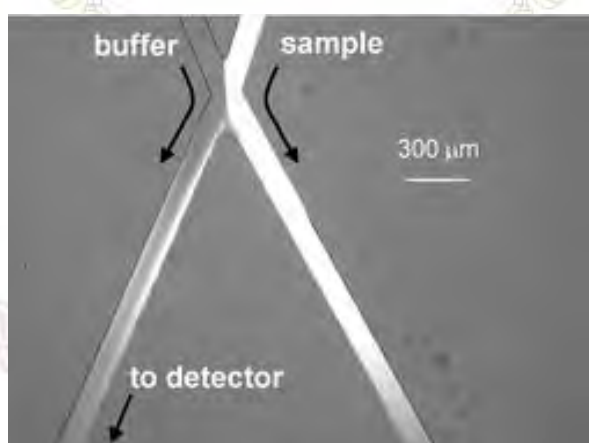


Figure 1.2 Electrochemical detection in laminar flow-based microfluidics. Reproduced from reference 14.

There have been many reports about electrochemical detection in microfluidic systems, but most of them have been focused on laminar-flow based microfluidics¹⁵⁻¹⁸. Few years ago, some researchers reported electrochemical detection for droplet-based microfluidics. Lou et al.¹⁹ presented gold microelectrodes to detect NaCl solution in a microfluidic system (Figure 1.3) and found that the limit of detection was as low as 0.02 mM. In addition, this detection system was used to measure conductivity of yeast cells which were encapsulated in aqueous droplets.

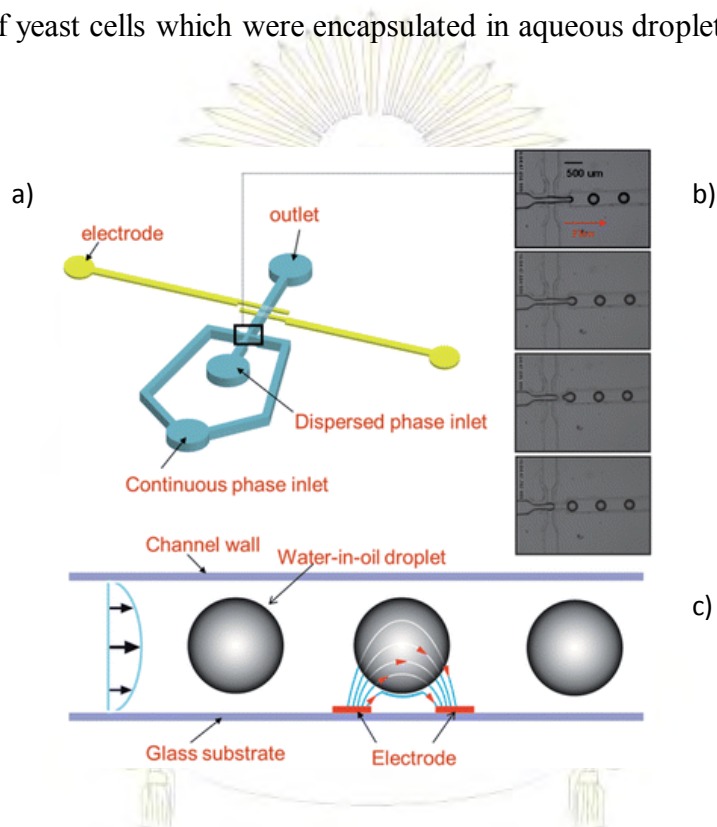


Figure 1.3 Electrochemical detection of droplets using amperometry (a) A pattern of microfluidic device (b) droplet generation (c) electrochemical measurements on each droplet. Reproduced from reference¹⁹.

Recently, Liu et al.²⁰ were developed amperometric detection using coupled microelectrodes to study reactions in each droplet. It was found that amperometric measurements depend on volume, water fraction of droplets and total flow rate of microfluidic systems. Experimental results were in agreement with the theory of Levich's equation. Additionally, they reported that the microelectrodes would solve detection in opaque materials of microdevices.

Han et al.²¹ presented an amperometric technique for studying enzyme behavior and reactions within aqueous droplets (Figure 1.4). Microelectrodes were put into microchannels. They found that the electrochemical detection showed high sensitivity when compared with fluorescence detection.

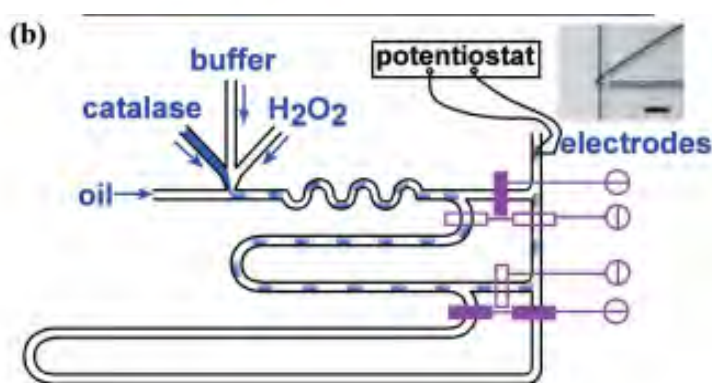


Figure 1.4 Amperometric detection for a droplet-based microfluidic system. The detection system consists of coupled microelectrodes incorporated with microdevices. Reproduced from reference 21.

There have been many articles reporting about developing of droplet-based microfluidics coupled with electrochemical detection using many patterns of channels and reservoirs for better resolution of detection²². However, there still have some problems about electrochemical detection for droplet-based microfluidics. For example, a microdroplet is too small for electrochemical detection and total flow rate of the system is too fast. Therefore, researchers have been tried to develop and design new approaches to solve these problems.

Lui and Crooks²³ reported a new method to improve electrochemical detection in droplet-based microfluidics using microbands gold electrodes as working, counter and reference electrodes. In addition, the width of the microchannel was decreased at the detection window, as seen in Figure 1.5. Accordingly, when microdroplets arrived at the narrow channel, they were elongated and slowed down. The elongated droplets passed across the microband electrodes slowly, resulting in sufficient analysis time for

an electrochemical process. This detection design has successfully shown to improve electrochemical detection in droplet-based microfluidic systems.



Figure 1.5 A microfluidic device with a narrow microchannel for elongation of droplets. Microband gold electrodes were placed across the narrow channel for detection of elongated droplets. Reproduced from reference 23.

1.6 Scope and Aims of this Work

From previous reports, especially Lui and Crooks' work, electrochemical method hold great promise for droplet detection. However, only a proof of concept has been reported in the previous work. There has not been an application in real sample. Therefore, in this work, an application of chronoamperometric detection in a droplet-based microfluidic system is demonstrated. Dopamine, a neurotransmitter and hormone in human, is used as a target analyte. Dopamine is also an electroactive species which can be detected using an electrochemical sensor. In addition, carbon paste electrodes (CPEs) are used in this system because CPE is one of the great electron transfer electrodes with a wide potential window and it is cheaper than metal electrodes.²⁴⁻²⁵ Therefore, droplet-based microfluidics with electrochemical detection using CPEs would be a high efficient platform for determination of dopamine.

Chapter 2

Theory

2.1 Droplet-based Microfluidics

Droplet-based microfluidics or segmented flow microfluidics is a novel system that was developed to solve the problems of laminar flow in microchannels. These problems cause slow mixing and the dispersion of solutes along the channels. Droplets generated in microfluidic systems are also called plugs and they can serve as reaction compartments with tiny volumes. Accordingly, small amount of samples and reagents is consumed by this microfluidic system.

2.1.1 Droplet generation

To form droplets, two immiscible solutions are required (generally oil and aqueous solutions). Oil is commonly used as a carrier phase (continuous phase). An aqueous solution is normally used as a dispersed phase that is broken into droplets by the carrier phase. For water-in-oil droplet systems, an oil phase is firstly pumped into a channel and an aqueous solution is then delivered into the system. When the aqueous phase meets the oil flow, the oil phase brakes the aqueous solution into droplets, as shown in Figure 2.1. Then, the droplets move along the microchannel with rapid mixing and no dispersion of the droplet contents.

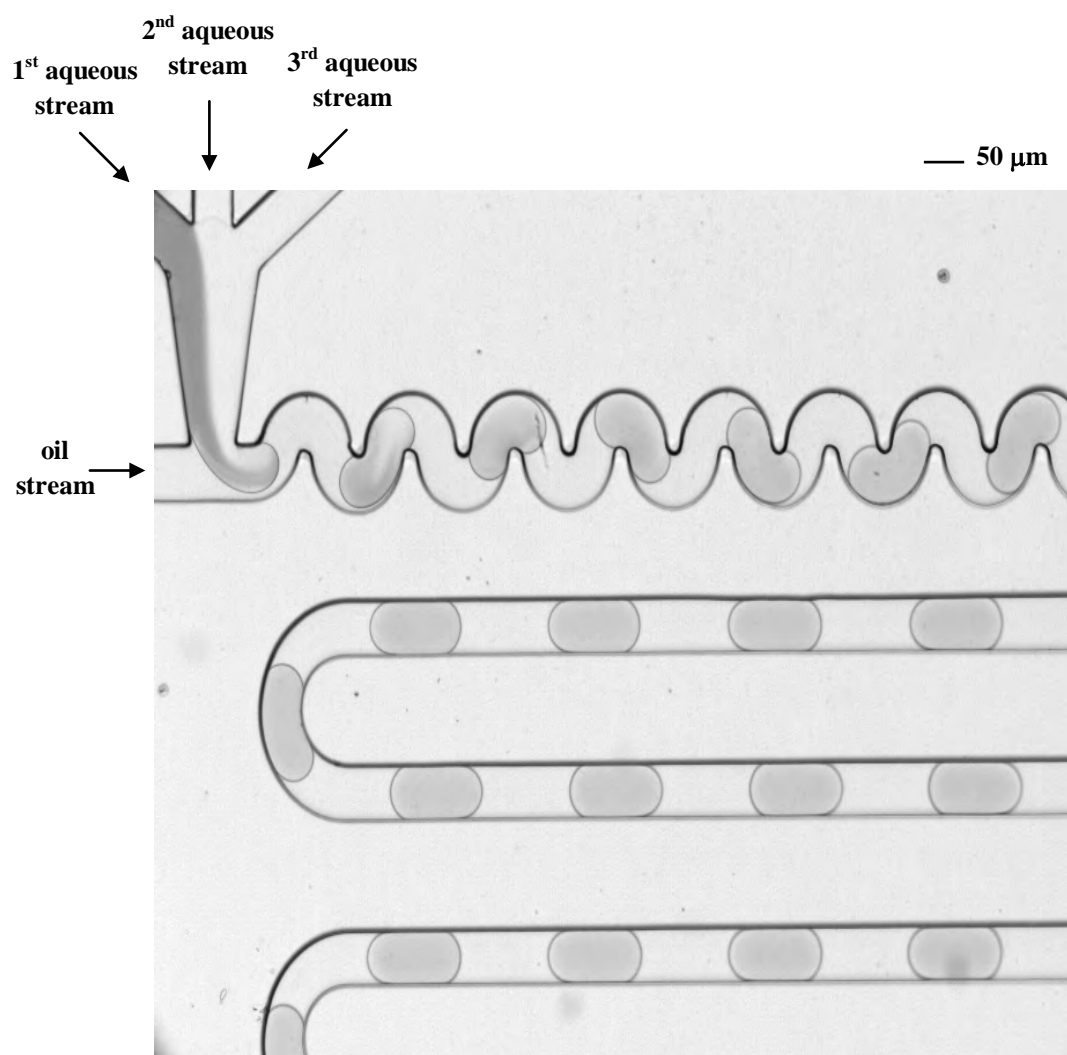


Figure 2.1 Droplet generation in a T-junction microfluidic device. Reproduced from reference 26.

There are many kinds of oil, such as vegetable oil²⁷ and perfluorodecaline (PFD).²⁸ PFD is widely used because it does not swell PDMS and is biocompatible.

To obtain clean transport of droplets along the microchannel, the carrier fluid, not the aqueous phase, must wet the walls of the microchannels. Accordingly, the surface tension at the water-PDMS interface has to be higher than the surface tension at the water-PFD interface. Therefore, 1*H*,1*H*,2*H*,2*H*-perfluoro-1-octanol as a surfactant is usually added into PFD to reduce the surface tension at the water-PFD interface.²⁸ Consequently, droplets move along the channel without leaving any footprints behind.

2.1.2 Droplet-size

Droplet size is important because it affects analysis time when monitoring reaction within droplets. Droplet size is related to water fraction (W_f) which is a significantly important parameter.

2.1.2.1 Water fraction

Water fraction (W_f) is a parameter that shows the fractions of water and oil phases in droplet generation. W_f can be calculated using the ratio of the total flow rate of an aqueous phase and the summation of the flow rate of aqueous and oil phases. The water fraction is calculated using the equation below;

$$W_f = \frac{F_w}{F_w + F_o} \quad (2.2)$$

where W_f is water fraction, F_w ($\mu\text{L}/\text{min}$) is flow rate of an aqueous phase and F_o ($\mu\text{L}/\text{min}$) is flow rate of a carrier phase. Water fraction is a parameter that strongly affects the droplet size. When the water fraction is higher, droplet size is larger, as seen in Figure 2.2. This is because more aqueous phase can come into droplets.

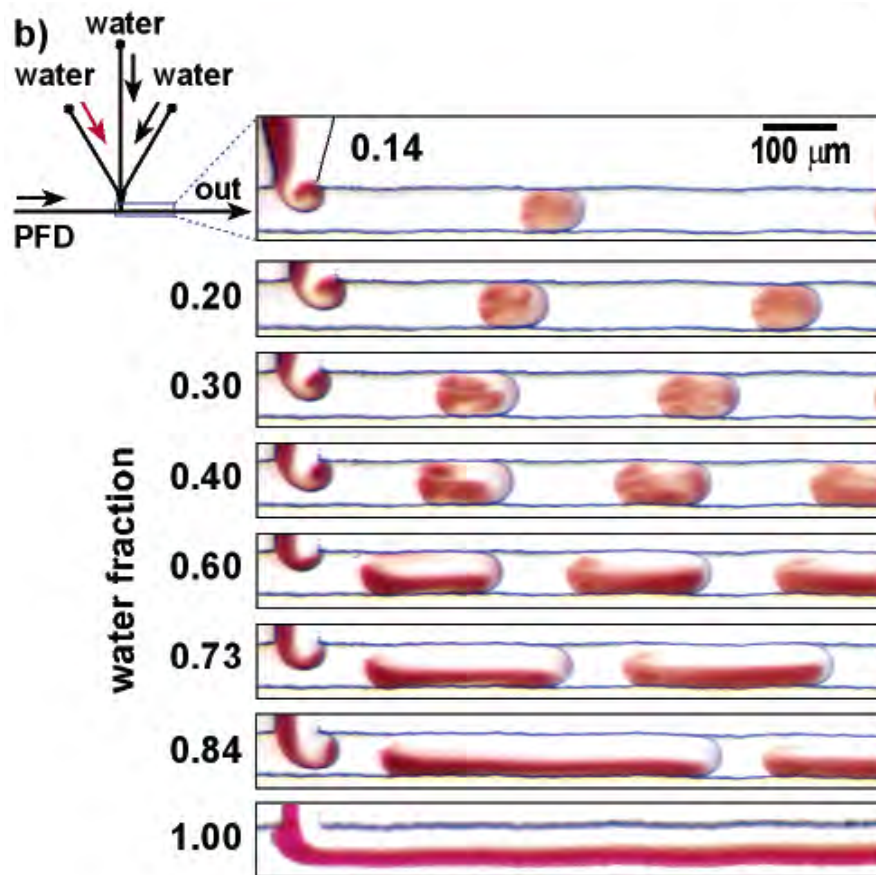


Figure 2.2 Droplet generation at different water fractions. Reproduced from reference 28.

If the value of W_f is too low, droplet formation may not be stable because low flow rates are used and a high precision pump is required to provide stable flow at low flow rates. In addition, if W_f is too high, droplets could be broken and the aqueous phase would wet channel. In addition, two parallel laminar flows would be observed instead of droplet formation if W_f is too high, as seen in Figure 2.2 at the W_f of 1.00.

2.1.3 Flow velocity

Flow velocity shows the speed of droplets travelling along the channel. The droplet size is independence of flow velocity, but flow velocity affects analysis time. Velocity of a droplet moving in the system can be calculated using the formula shown in Equation 2.3;

$$V_T = (F_T A) \frac{10^6}{60} \quad (2.3)$$

where V_T (mm/s) is droplet velocity, F_T ($\mu\text{L}/\text{min}$) is total flow rate in the system which is the summation of flow rate of all inlets and A (mm^2) is droplet area in a microchannel. Flow velocity affects analysis time. When flow velocity is too fast, the detector may not be able to measure the droplet contents effectively. Furthermore, too slow velocity would generate unstable droplets in the system, which may affect accuracy and precision of the measurements.

2.1.4 Mixing in droplet

Mixing of solutions is very important, especially in kinetic studies. Slow mixing can cause the reactions not complete before detection. Rapid mixing in droplets can be achieved using a curved channel, which is a part of the channel network. When a straight channel is replaced with a winding channel, the reorientations of droplet contents are repeated continuously. There are stretch and fold mechanisms in each droplet²⁹ (Figure 2.3). When a plug is moving through a curve channel, its content is mixed chaotically, resulting in rapid mixing in droplets. However, a winding channel does not help rapid mixing in laminar flow, as shown in Figure 2.4. Therefore, a winding channel only enhances mixing in droplet systems.³⁰⁻³¹

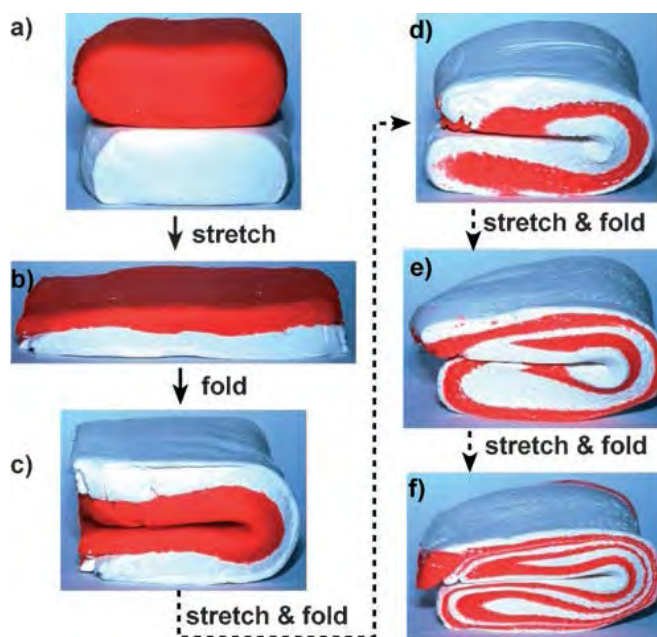


Figure 2.3 A model to explain the mixing of two reagents by chaotic advection; Photographs of two layers of the modeling clay being stretched and folded. Reproduced from reference 29.

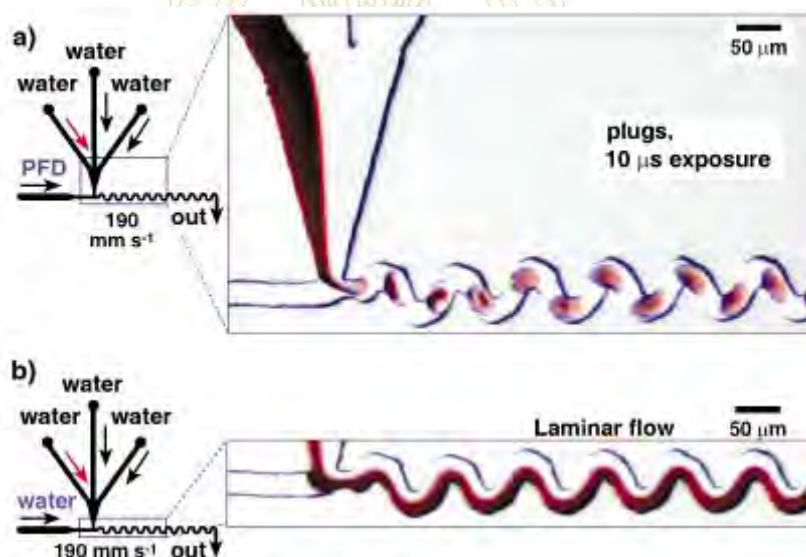


Figure 2.4 Comparison of a) laminar flow microfluidics and b) droplet-based microfluidics. The droplet system exploits a winding channel to generate rapidly chaotic mixing. Reproduced from reference 3.

2.2 Microchip Fabrication

Fabrication of microfluidic devices is normally used soft lithography. AutoCAD is commonly used for designing patterns of microchannels of microchips or microfluidic devices. After that, SU-8 photoresist is molded on a silicon wafer to generate a master template according to the designed pattern. Then, a monomer of polydimethylsiloxane (PDMS) mixed with a curing agent is poured onto the master and allowed the polymer to be cured in an oven at 65 °C for 2-6 hours. A PDMS replica is then peeled from the master. Finally, the PDMS replica is bonded with another PDMS plate or glass to enclose the channels. Summary of microfluidic device fabrication is shown in Figures 2.5 (a)-(e). The fabrication process is explained in more detail in Section 3.2.

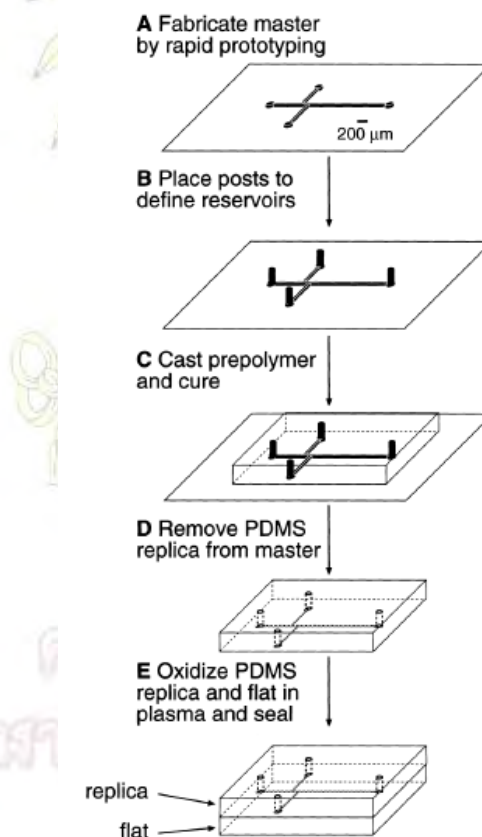


Figure 2.5 Microchip fabrications (a) a design (using AutoCAD) printed on a film mask (b) making of reservoirs (c) PDMS casting (d) removal of a PDMS replica (e) PDMS bonding to enclose the system. Reproduced from reference 32.

2.3 **Electrochemical Detection**

Electrochemical detection is one of the most useful methods for determining the amount of analytes. Advantages of electrochemical detection include low limit of detection, good sensitivity, good accuracy, portability and low cost. Moreover, the size of electrochemical instruments is more suitable with microfluidic systems than traditional fluorescence setups. There are many techniques of electrochemical measurements, such as potentiometry, voltammetry and amperometry.³³ In this work, only cyclic voltammetry and chronoamperometry are exploited.

2.3.1 **Cyclic voltammogram**

For cyclic voltammetry, potentials are scanned to measure currents and the currents are then plotted against the potential to generate a cyclic voltammogram. The cyclic voltammogram shows the working potential that gives the highest current. In addition, a cyclic voltammogram shows a working potential range that can be used for measurements and may predict a suitable applied potential for amperometric measurements. Cyclic voltammograms, in this work, are generated using square wave voltammetry which gives high sensitivity and selectivity compared to other electrochemical techniques. A typical cyclic voltammogram is shown in Figure 2.6.

ภาควิชาเคมี
คณะวิทยาศาสตร์
จุฬาลงกรณ์มหาวิทยาลัย

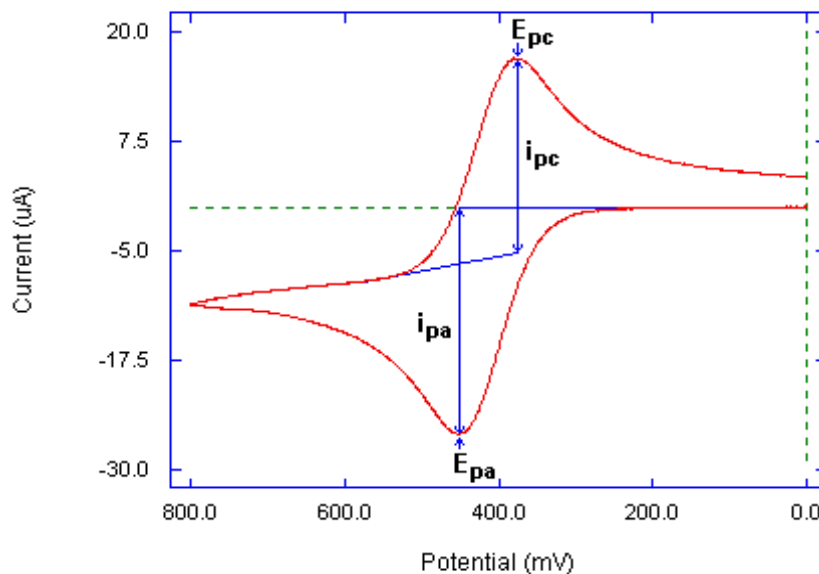


Figure 2.6 A typical cyclic voltammogram. E_{pc} is cathodic peak potential, i_{pc} is cathodic peak current, E_{pa} is anodic peak potential and i_{pa} is anodic peak current. Reproduced from reference 35.

2.3.2 Chronoamperometric detection

Chronoamperometry is used to measure current with time when an applied potential is fixed. The current is a result of electrochemical oxidation (positive applied potential) or reduction (negative applied potential) of electroactive compounds after applying a potential pulse across the working and auxiliary electrodes. In chronoamperogram, the initial peak current is high and then decreases exponentially with time until reaches the steady state³⁶. A hydrodynamic voltammogram, a plot of applied potential versus signal to noise ratios of currents, is normally generated to find the optimum applied potential for chronoamperometric measurements, as shown in Figure 2.7.

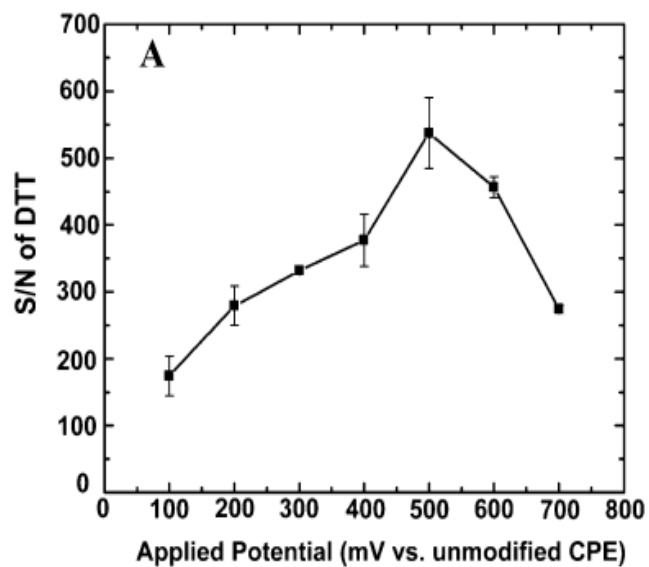



Figure 2.7 Hydrodynamic voltammogram plotted using the signal-to-noise ratio as a function of the applied potential of 100 μ M Dithiotheritol injection. Reproduced from reference 25.



Chapter 3

Methodology

3.1 Chemicals and Equipment



Chemicals	Companies
1.Noujol Mineral oil	Perkin Elmer (Thailand)
2.Graphite powder ($\leq 20 \mu\text{m}$)	Sigma-Aldrich (Singapore)
3.Elastomer kit (Slygard 184)	Dow Corning (Midland, MI)
4.Silver paint	SPI supplied (Wast Chester, PA, USA)
5.Perfluorodecalin (95%)	Sigma-Aldrich (Singapore)
6.1 <i>H</i> ,1 <i>H</i> ,2 <i>H</i> ,2 <i>H</i> -perfluoro-1-octanol	Sigma-Aldrich (Singapore)
7.Dopamine hydrochloride	Sigma-Aldrich (Singapore)
8.Ascorbic acid (99.7%)	BDH (AnalaR, England)
9.Domine-250 (dopamine 250 mg/10 mL)	Modernmanu (Bangkok, Thailand)
10.UPAMINE (dopamine 250 mg/10 mL)	UMEDA (Bangkok, Thailand)
11.DOPAMEX (dopamine 200 mg/10 mL)	BIOLAB (Samutprakarn, Thailand)
12.Vitamin C (500 mg/2 mL)	Atlantic Lab. (Bangkok, Thailand)
13.NaCl	Merck (USA)
14.KCl	Ajax Finechem (Thailand)
15.Na ₂ HPO ₄	Merck (USA)
16.KH ₂ PO ₄	Carlo ERBA (Thailand)
17.Deionized water (Milli-Q Gradient)	Millipore (Thailand)
18.Ethanol	Merck (Germany)

Equipment	Companies
1.Potentiostat (ED410, 410-088)	eDAQ,(Australia)
2.Syringe pump (Harvard Apparatus 11)	Harvard Apparatus (USA)
3.Wires (AWG: 22, 100 FT.)	ALPS Industrial (Thailand)
4.Microscope (SZ-PT)	Olympus (Japan)
5.Tubing (OD: 1.09 mm, ID: 0.38 mm)	Portex (UK)
6.Syringe (1 mL)	Nipro (Thailand)
7.safe-lock-tube (1-2 mL)	Eppendorf (Thailand)
8.Micropipettes (10, 100, 1000 μ L)	Eppendorf (Thailand)

3.2 Device Fabrication

3.2.1 PDMS mold fabrication

A PDMS mold or SU-8 master was fabricated onto a silicon wafer using SU-8, a negative photoresist, to serve as a mold for PDMS microfluidic device fabrication. This fabrication process was done by Nipapan Ruecha at the department of Chemistry, Colorado State University, USA. Briefly, the mold was fabricated by pouring 1 mL of SU-8 (3050) onto a silicon wafer. The silicon wafer with SU-8 was then spun using a particular spin speed to obtain a desired thickness of an SU-8 layer. For example, for a thickness of 100 μ m of SU-8 3050, two spinning steps were required. Firstly, a spin speed at 500 rpm was used with an accelerating rate of 100 rpm and hold at this speed for 10 seconds and then the speed was increased to 1,000 rpm with an accelerating rate of 300 rpm and hold at this speed for 30 seconds. After that, the SU-8 coated wafer was dried by soft baking at 95 °C for 45 minutes to remove the solvent. A film mask with channel structures, designed using AutoCAD 2010, was then placed onto the silicon wafer coated with SU-8. The coated silicon wafer covered with the film mask was exposed under UVlight for 90 seconds to transfer the microchannel pattern from the film mask onto the coated silicon wafer. The UV-light initiates polymerization of the exposed SU-8. After the UV exposure, post baking was required for the cross-linking process of the UV exposed SU-8, resulting in solid SU-8 structures. The exposed silicon wafer was baked at 65 °C for 1 minute and 90 °C for 15 minutes. The patterned silicon wafer was then developed by being immersed into 50% (v/v) propylene glycol and monomethyl ether acetate for 20

minutes to remove un-exposed SU-8 on the silicon wafer. After rinsing with acetone and being dried with nitrogen gas, the silicon wafer was then placed in an oven at 90 °C for 15 minutes. Finally, the patterned silicon wafer with SU-8 was obtained to serve as a PDMS mold or SU-8 master, as shown in Figure 3.1, to fabricate microfluidic devices. All steps of the SU-8 master fabrication are depicted in Figure 3.2.

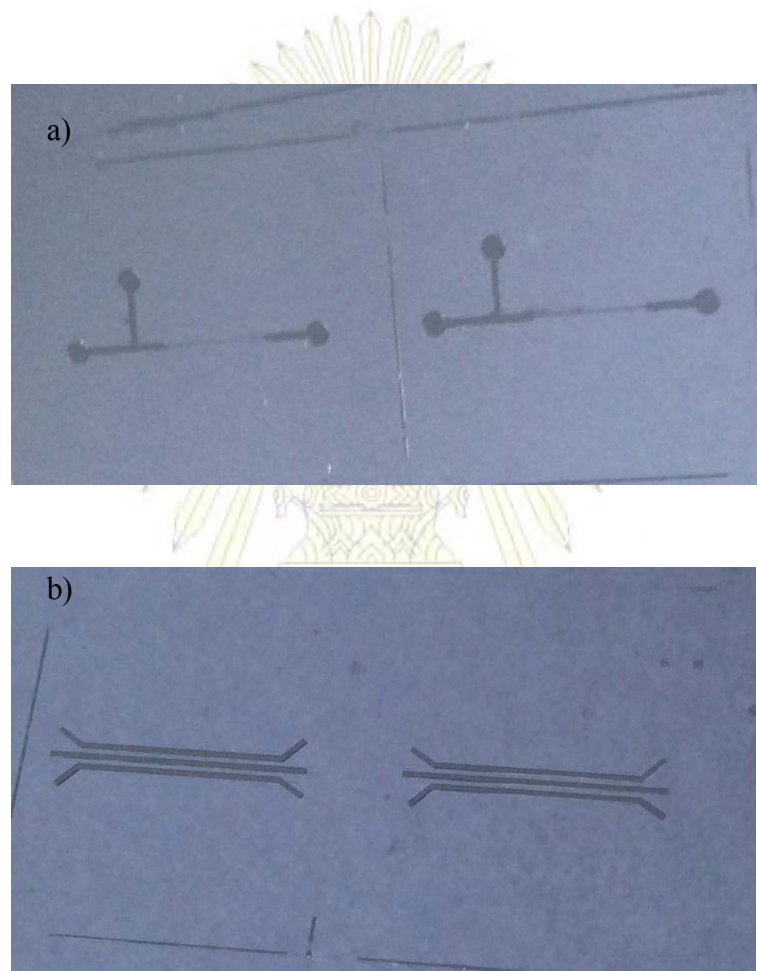


Figure 3.1 Complete SU-8 masters on silicon wafer a) microchannel patterned and b) electrode patterned masters.

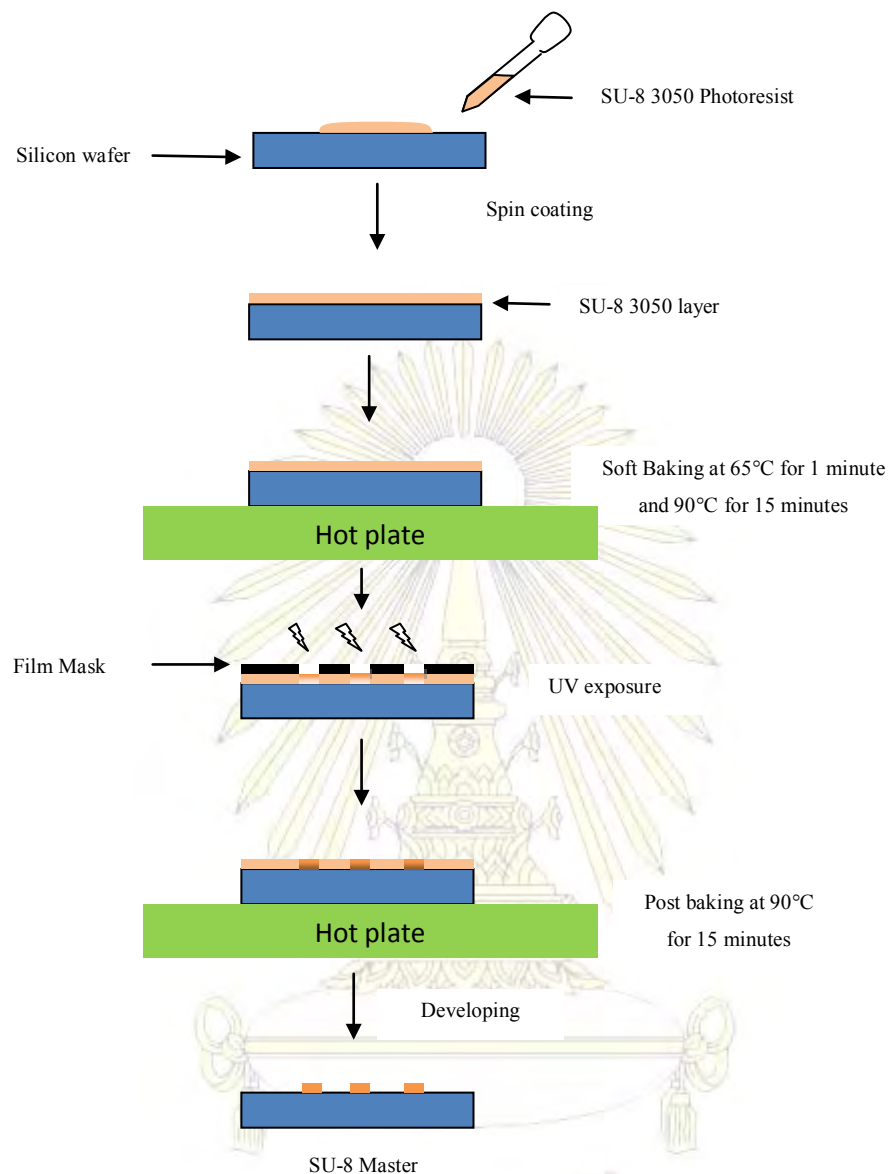


Figure 3.2 Fabrication process of a PDMS master using an SU-8 photoresist.

3.2.2 PDMS casting

A PDMS mold was cleaned using n-hexane, methanol and ethanol with sonication for 10, 5 and 5 minutes, respectively. Aluminum foil was used to wrap the PDMS mold to make a container (as shown in Figure 3.3). The PDMS monomer and curing agent were mixed a weight ratio of 10:1. The mixture was degassed in a vacuum desiccator for 30 minutes to remove gas bubbles and then poured onto the

PDMS mold. After that, the PDMS mold was cured at 65 °C in an oven for 2-6 hours. A PDMS replica was peeled from the mold and cleaned using nitrogen gas. There are two types of PDMS replica; channel patterned and electrodes patterned PDMS (Figure 3.4). The PDMS casting process is shown in Figure 3.3.

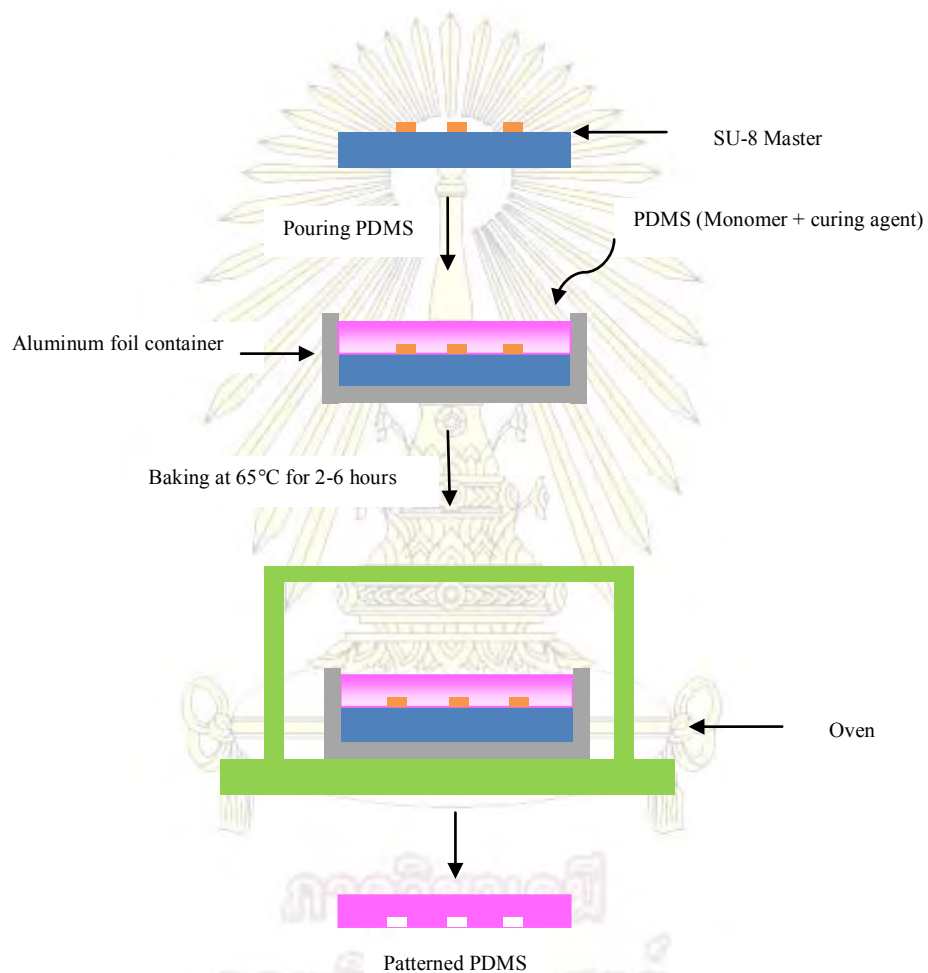


Figure 3.3 Summary of a PDMS casting process for microfluidic device fabrication.

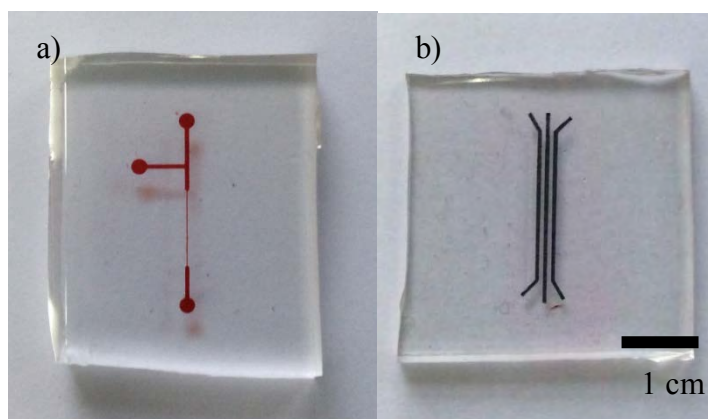


Figure 3.4 PDMS replicas; a) microchannel patterned PDMS and b) electrode patterned PDMS. A red dye was filled into the channel in a) for visualization.

3.2.3 Electrode fabrication

Electrodes used in this work are carbon paste electrodes (CPEs) mixed with PDMS. These electrodes were incorporated into a PDMS microfluidic device. To fabricate electrodes, firstly, 0.91 g PDMS elastomer and 0.09 g curing agent were blended with 1.0 g noujol oil until the mixture was turbid. Secondly, 2.0 g graphite powder was added into the mixture and the electrode paste is ready to use (Figure 3.5). Thirdly, the paste was spread into the channels of a PDMS plate patterned for electrodes (Figures 3.6-3.7). Before spreading the paste, Scotch Magic Tape™ was applied around the electrode channels (Figure 3.6) to act as a border of the paste for easy cleaning. Excess paste was removed using a scraper to wipe over the electrode channels (Figure 3.8). Finally, the patterned electrodes were left for overnight before use. The complete electrodes are shown in Figure 3.9. There are three electrode channels, which represent working, counter and reference electrodes. The electrodes are 100 μm in depth and 500 μm in width. The space between each electrode is 500 μm .

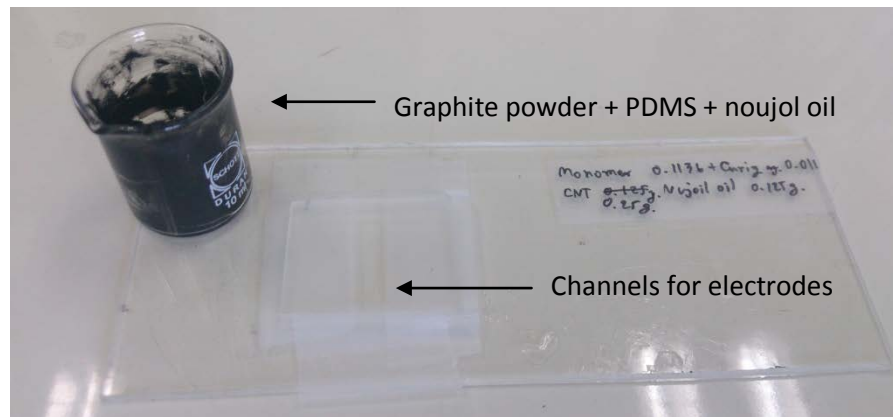


Figure 3.5 The paste for electrode fabrication and an electrode-patterned PDMS plate.



Figure 3.6 The electrode paste was filled into the channels on a PDMS plate.

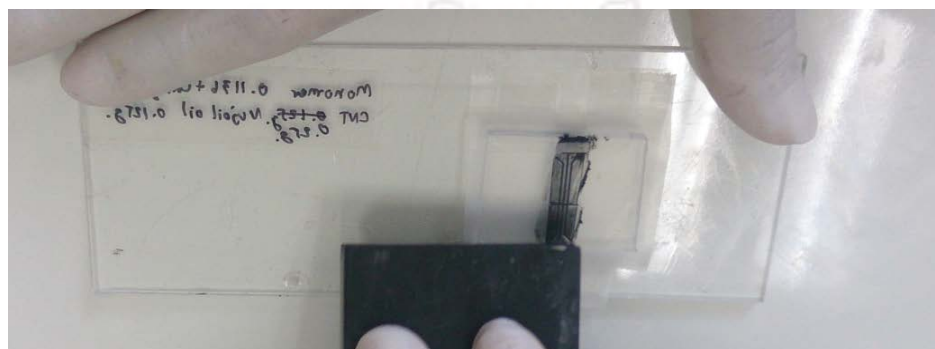


Figure 3.7 The electrodes paste was spread to fill the microchannels.

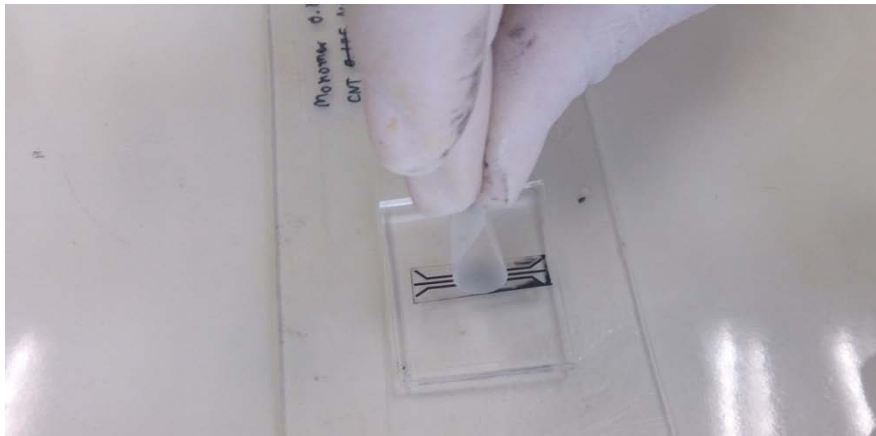


Figure 3.8 Removal of excess electrode paste using Scotch Magic Tape™.

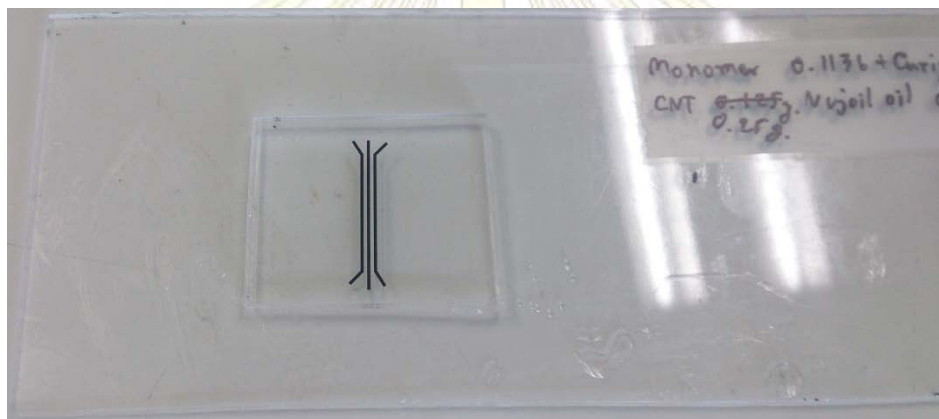


Figure 3.9 The patterned CPEs on a PDMS plate.

3.2.4 PDMS microchip assembly

After leaving the electrodes to be stable, the electrode-patterned PDMS plate was bonded to a channel-patterned PDMS plate to make a closed channel system. Before bonding, the PDMS plate with designed channel layout was punched to make holes (using a puncher) to serve as a fluidic interface between the microdevice and macro-scale reservoirs. The punched PDMS plate was first cleaned using nitrogen gas and then ready to be seal together with the electrode-patterned PDMS plate. Oxygen plasma, an irreversible sealing method, is commonly used to bond PDMS plates

together. This method was performed by placing both PDMS plates into a plasma oven. The PDMS plates were exposed to the plasma at a high level for 1 minute. Later, one PDMS plate was placed on top of the other for bonding. In this study, oxygen plasma was found to cause the decomposition of noujol oil, which is a soft component of the electrodes. This decreases sensitivity of the electrodes. Accordingly, reversible sealing using ethanol was used to solve this problem. To do the reversible bonding, both PDMS plates (electrode-patterned and channel-patterned), were cleaned with nitrogen gas. Ethanol was then dropped onto both PDMS plates. After that, the PDMS plate with patterned channels was placed carefully onto the electrode patterned PDMS plate to obtain a complete microfluidic device. Finally, the complete microchip was placed in a 65°C oven for 1 hour.

3.2.5 **Electric wire connection**

Electric wires were attached to each electrode of the sealed microchip to make connections (Figure 3.10). Before attaching the wires, the part of electrodes that is not covered by the PDMS plate and not used for connection was removed for preventing the electrical short. Silver paste was then glued as a connector between each electrode and its wire (Figure 3.11). Finally, epoxy glue was applied to the connection area between the electrode and its wire for electrode protection, long-lasting and reducing background noise. Figure 3.12 shows a complete microfluidic device with patterned channels (500 μm width and 100 μm depth). This device consists of a T-junction with two inlets and one outlet. The main channel of 500 μm width was confined into a narrow section of 50 μm width for electrochemical detection of droplets. The patterned CPEs were in a cross position with the narrow channel.

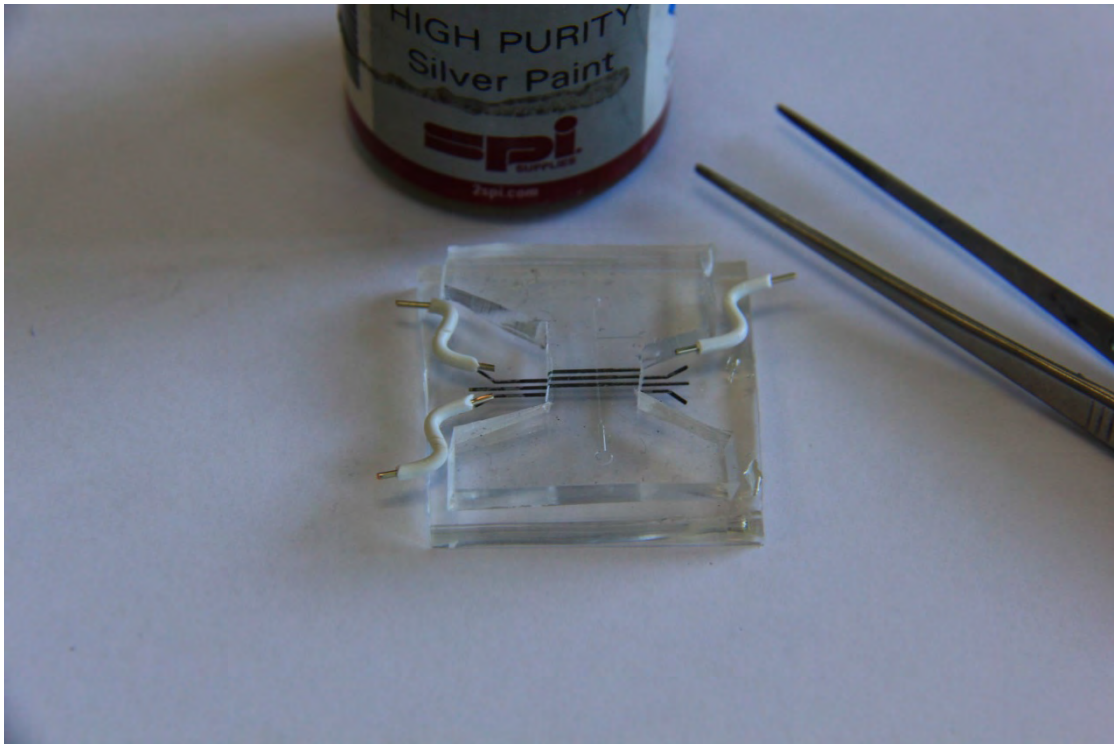


Figure 3.10 Connection of wires to the electrodes.

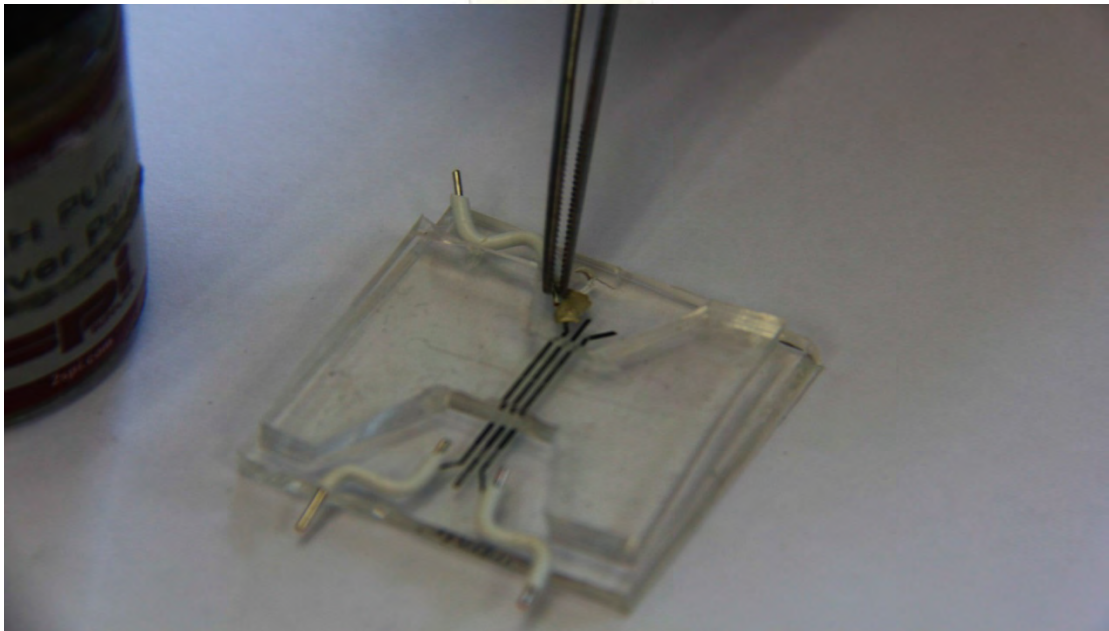


Figure 3.11 Silver paste as a connector between the wires and electrodes.

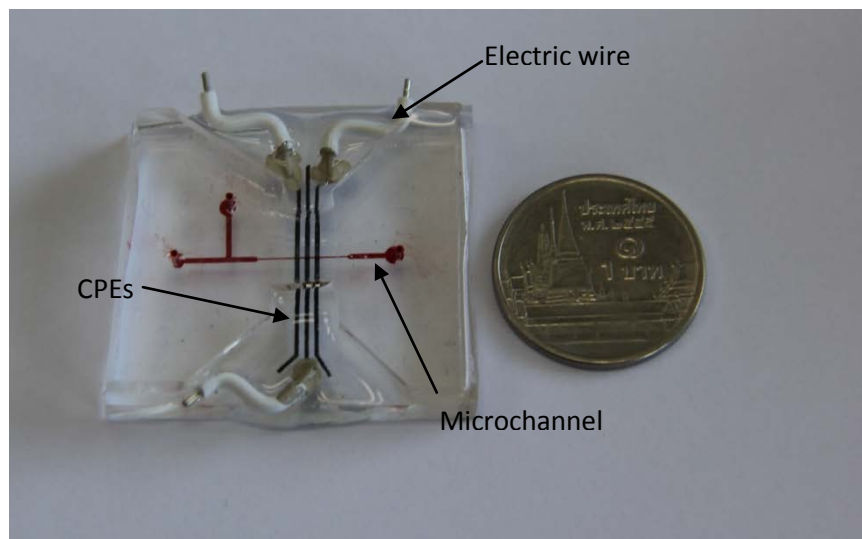


Figure 3.12 A complete microfluidic device for electrochemical detection.

3.3 Preparation of Solutions

3.3.1 Phosphate buffer saline

Phosphate buffer saline (PBS), pH 7.4, at a concentration of 0.1 M was used as a supporting electrolyte for all experiments. To prepare 0.1 M PBS, 2.0 g NaCl, 0.05 g KCl, 0.36 g Na₂HPO₄ and 0.06 g KH₂PO₄ were dissolved in a 250 mL volumetric flask using deionized water (18.0 MΩ cm, Milli-Q Gradient System, Millipore). This 0.1 M PBS was used to prepare all aqueous solutions.

3.3.2 Standard solutions of dopamine (DA) and ascorbic acid (AA)

Dopamine hydrochloride and ascorbic acid stock solutions at a concentration of 80 mM were prepared separately by dissolving 15.17 mg dopamine and 14.09 mg ascorbic acid in 1 mL of 0.1 M PBS in safe-lock tubes. A concentration series of both DA and AA were prepared separately in safe-lock tubes at 0.5, 1.0, 1.5, 2.0, 2.5, 3.0, 5.0 and 8.0 mM by pipetting from 80 mM stock solutions. The volumes of pipetting to prepare each concentration are shown in Table 3.1. Finally, 0.1 M PBS was used to adjust the final volume to be 1 mL.

Table 3.1 Volumes of stock solutions pipetted to prepare a concentration series of DA and AA.

Concentration (DA & AA) (mM)	Volume of pipetting (μL)	PBS volume (μL)	Total volume (μL)
0.5	6.25	993.75	1,000
1.0	12.50	987.50	1,000
1.5	18.75	981.25	1,000
2.0	25.00	975.00	1,000
2.5	31.25	968.75	1,000
5.0	62.50	937.50	1,000
8.0	100.0	900.00	1,000

3.3.3 Sample solutions

Real samples of DA (Domine-250, UPAMINE, and DOPAMEX) and AA (Atlantic lab) were prepared at concentrations of 1.0 and 1.5 mM, respectively. Pipetted volumes of each real sample are shown in Table 3.2. All solutions were then adjusted the final volume to be 2 mL using 0.1 PBS solutions in safe-lock tubes.

Table 3.2 Volumes of pipetted real samples to prepare DA and AA sample solutions at concentrations of 1.0 and 1.5 mM, respectively.

Sample	Brand name	Concentration (mM)	Volume of pipetting (μL)	Volume of PBS (μL)	Total volume (μL)
DA	Domine-250 (250 mg/ 10 mL)	1.00	15.70	1984.30	2,000
DA	UPAMINE (250 mg/ 10 mL)	1.00	15.70	1984.30	2,000
DA	DOPAMEX (200 mg/ 10 mL)	1.00	18.92	1981.08	2,000
AA	Atlantic lab. (500 mg/ 2 mL)	1.50	4.26	1995.74	2,000

3.4 Experimental Setup

3.4.1 Electrochemical performance

To test the performance of the chip-based CPEs, Cyclic voltammetry was used. This batch experiment was performed using a microfluidic device designed to have a small well (1 cm i.d.) covering the three-band electrodes, as shown in Figure 3.13. In this experiment, linear sweeping voltammetry was used for measurements of 1 mM DA using a pulse amplitude of 0.15 V, a square wave frequency of 30 Hz and a step height of 0.005 V for scanning the potentials between -0.2 V and 0.8 V versus carbon pseudo-reference electrode.

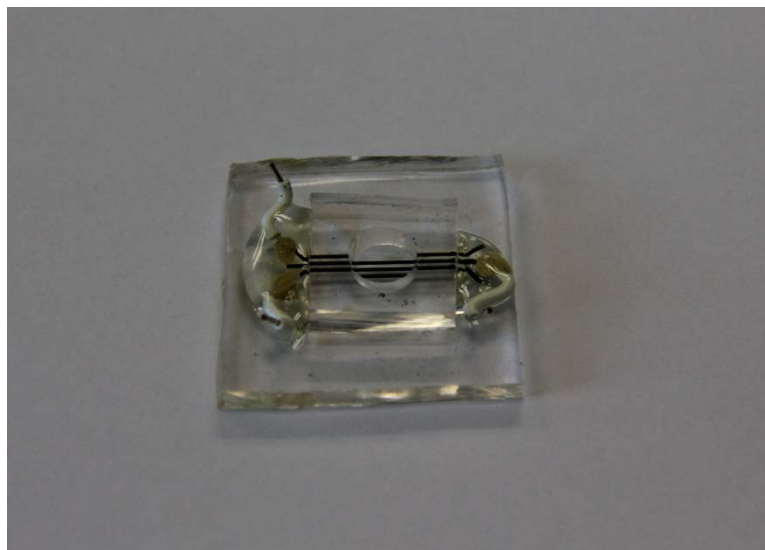


Figure 3.13 A microfluidic device for batch measurements. The device has a small well with 1 cm i.d. covering the CPEs.

3.4.2 **Droplet generation**

In this work, droplets were generated using a T-junction microfluidic device (as shown in Figure 3.12). An Oil phase or carrier phase, was prepared by mixing perfluorodecalin with 1*H*, 1*H*, 2*H*, 2*H*-perfluoro-1-octanol, as a surfactant, at a ratio of 10:2 (v/v). To generate droplets, the oil phase filled in a 1 mL plastic syringe was pumped using a syringe pump through tubing, which is used as a connection between the syringe and the device inlet, into the microfluidic device for 10 minutes. The oil flow was for developing hydrophobicity of the microchannel surface. After that, an aqueous phase, stored in another 1 mL plastic syringe, was delivered to the other inlet, which is perpendicular to the oil inlet, using another syringe pump. When the aqueous phase flowed into the T-junction, the oil phase broke the aqueous solution into droplets. The experimental setup is shown in Figure 3.14. The microfluidic device was placed on a microscope for visualization.

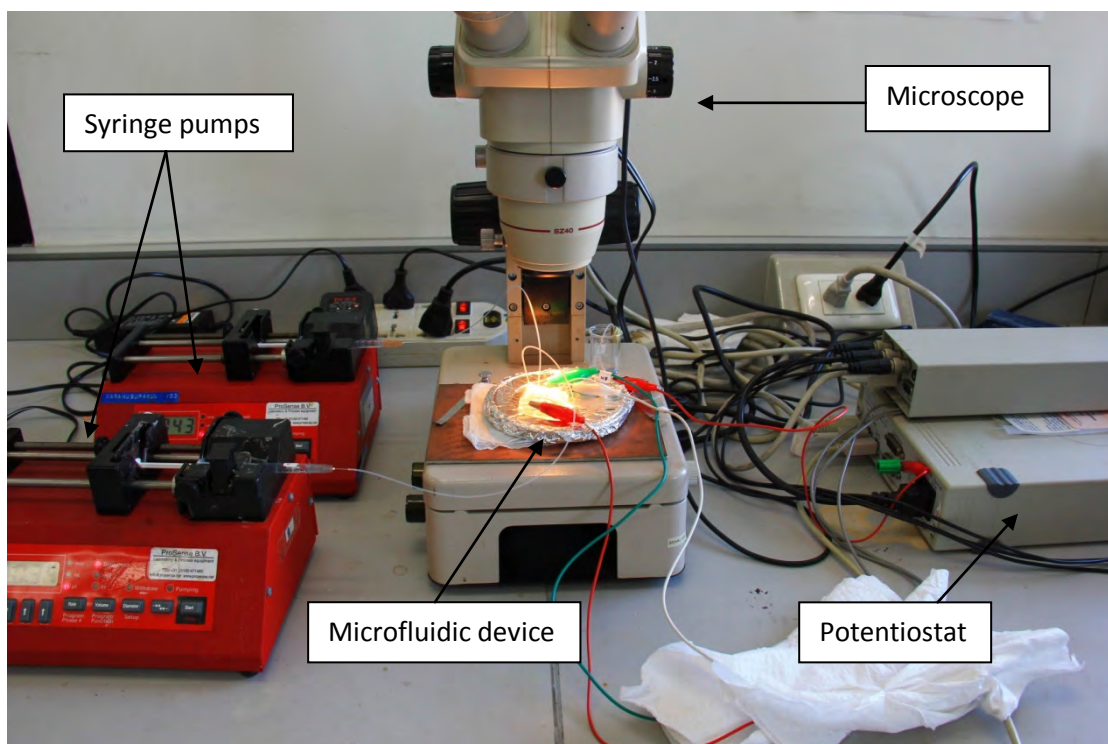


Figure 3.14 The experimental set up of a droplet-based microfluidic device with electrochemical detection. The device is placed on microscope stage for visualization.

3.4.3 Chronoamperometry in microdroplet

3.4.3.1 Hydrodynamic voltammogram

Hydrodynamic voltammograms were generated to find an optimum applied potential, which is given the highest S/N of current, for chronoamperometry. Flow rates of 1.8 and 0.8 $\mu\text{L}/\text{min}$ were applied for the oil phase and aqueous solutions, respectively. In this work, 1.0 mM DA in 0.1 M PBS was used to generate droplets for hydrodynamic measurements. To perform the experiments, 0, 50, 100, 150, 200, 250, 300, 350, 400, 450 and 500 mV potentials were applied and data was then collected for 1 minute. After that, averaged currents were plotted versus applied potential to generate hydrodynamic voltammograms.

3.4.3.2 Effect water fraction (W_f)

Water fraction (W_f), which is given by $W_f = F_w / (F_w + F_o)$ where F_w is aqueous flow rate and F_o is oil flow rate, is an important parameter to control droplet size. To study of effect of W_f on chronoamperometric measurements in droplets, total flow rate was fixed at 2.6 $\mu\text{L}/\text{min}$. The W_f was varied from 0.15 to 0.46 to generate droplets with different sizes. Flow rates for each inlet are shown in Table 3.3.

Table 3.3 Flow rates applied to each inlet to study effect of W_f .

Oil ($\mu\text{L}/\text{min}$)	Aqueous ($\mu\text{L}/\text{min}$)	Total ($\mu\text{L}/\text{min}$)	Water fraction (W_f)
1.40	1.20	2.60	0.46
1.60	1.00	2.60	0.38
1.80	0.80	2.60	0.31
2.00	0.60	2.60	0.23
2.20	0.40	2.60	0.15

3.4.3.3 Effect of total flow rate

Another parameter for chronoamperometry in microdroplets is total flow rate. If flow rate is too fast, the sensor cannot detect the droplet contents. On the other hand, if flow rate is too slow, sample through-put is low and droplet generation might not be stable. Here, total flow rates were varied, but the W_f was fixed at 0.31. Flow rates applied to each inlet are shown in Table 3.4.

Table 3.4 Flow rates applied to each inlet to study effect of total flow rate on chronoamperometry in droplets.

Oil ($\mu\text{L}/\text{min}$)	Aqueous ($\mu\text{L}/\text{min}$)	Total ($\mu\text{L}/\text{min}$)	Water fraction
0.90	0.40	1.30	0.31
1.35	0.60	1.95	0.31
1.80	0.80	2.60	0.31
2.25	1.00	3.25	0.31
2.70	1.20	3.90	0.31

3.5 Method of Validation

3.5.1 Calibration curve

To construct calibration curves of DA and AA, a concentration series of DA and AA from 0.5-8.0 mM were prepared, as shown in Table 3.1. Each concentration was used to generate droplets and currents arising from the droplet contents were measured for 1 minute. After that, averaged currents were plotted versus the concentration to construct calibration curves.

3.5.2 Linearity

In this work, linearity was determined from calibration curves and then the concentration was increased until the current was out of the straight line. After that, the concentration was decreased until the current was out of the straight line. In addition, the relative coefficient (R^2) was used to determine the linear range.

3.5.3 Limit of detection (LOD) and limit of quantitation (LOQ)

Limit of detection and limit of quantitation were measured after constructing calibration curves. To obtain LOD and LOQ, the concentrations of DA and AA were decreased until S/N values equal to 10 and 3 for LOQ and LOD, respectively, then these concentrations were rechecked with the calculated values, which are determined by 3 times of standard deviation (SD) of the background for LOD and 10 times for LOQ.

3.5.4 Precision

Intraday precision was determined in one day using 3 concentrations of analytes (0.5, 1.5 and 2.5 mM). For each concentration, 50 droplets were measured. Percentages of the relative standard deviation (%RSD) were then calculated using the equation below;

$$\%RSD = \frac{SD}{\bar{x}} \times 100 \quad (3.1)$$

where SD is standard deviation and \bar{x} is averaged current.

Inter-day precision was measured using 1.5 mM of analytes. In this work, the experiments were carried out for 3 days (in the same week). From averaged currents, %RSD and %error (Equation 3.2) were calculated to determine inter-day precision.

$$\%Error = \frac{(C_{det} - C_{labeled})}{C_{labeled}} \times 100 \quad (3.2)$$

where C_{det} is determined concentration and $C_{labeled}$ is labeled concentration.

3.6 Sample Measurements

Prepared samples from Table 3.2 were used to generate droplets using flow rates of oil and aqueous solutions to be 1.8 and 0.8 $\mu\text{L}/\text{min}$, respectively. The droplet contents were measured for currents using an applied potential of 150 mV. After that, the determined amount was compared with the labeled amount and the error percentages were calculated to evaluate the accuracy of the droplet systems.



Chapter 4

Results and Discussion

4.1 Electrochemical Performance

4.1.1 Cyclic voltammogram

To study sensor performances, cyclic voltammetry was used as a tool to characterize the CPEs. Cyclic voltammograms were generated from batch measurements. Effect of the bonding method between the irreversible plasma bonding and reversible ethanol bonding to the electrochemical performance of the CPEs was investigated. First, microfluidic devices bonded using the irreversible plasma-bonding and reversible ethanol bonding were used to generate cyclic voltammograms of 0.1 mM DA. A cyclic voltammogram obtained from the oxygen-plasma bonding device (Figure 4.1 (a)) shows lower currents of 1 mM dopamine when compared with the reversible bonding device (Figure 4.1 (b)). This is because the oxygen-plasma bonding (irreversible method) was found to decompose the noujol oil (soft component) in the carbon paste electrodes, causing low sensitivity of the electrodes.

ภาควิชาเคมี
คณะวิทยาศาสตร์
จุฬาลงกรณ์มหาวิทยาลัย

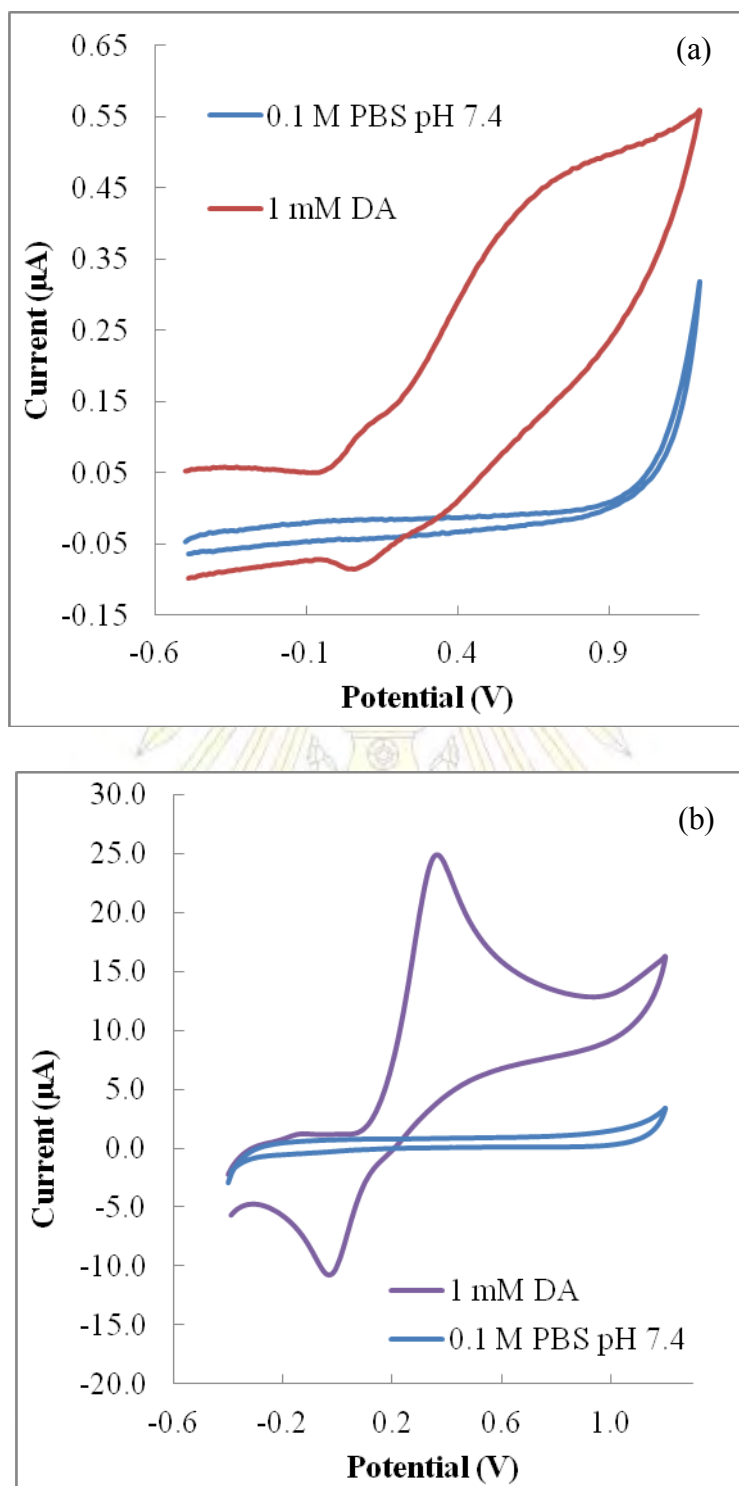


Figure 4.1 Voltammograms of 0.1 mM dopamine in 0.1 M PBS (pH 7.4) generated using (a) irreversible oxygen plasma bonding (b) reversible ethanol bonding devices.

In addition, the voltammogram of the plasma bonding method (Figure 4.1 (a)) is irreversible while the voltammogram of the ethanol bonding (Figure 4.1 (b)) is quasi-reversible. Moreover, for plasma bonding, the potential which gives the highest current is shifted to nearly a hydrogen evolution potential, which may disturb the measurement. After that, a cyclic voltammogram of 1 mM ascorbic acid was generated using the same way as that of dopamine. A cyclic voltammogram of AA was irreversible with no appearance of cathodic peak current. Compared results are shown in Figure 4.2.

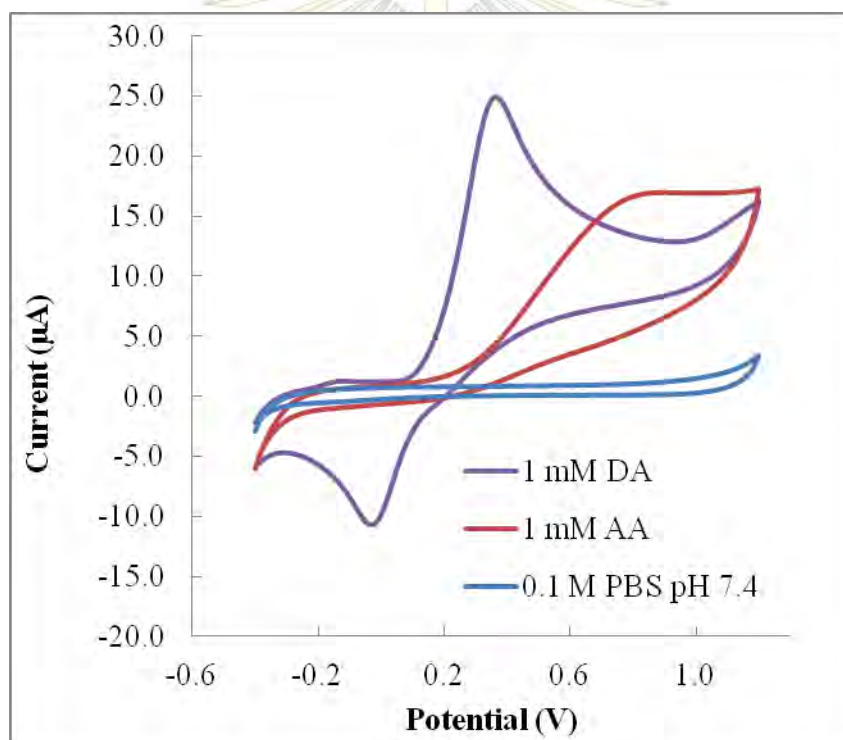


Figure 4.2 Cyclic voltammograms of dopamine and ascorbic acid when generated using the reversible bonding chip.

The cyclic voltammogram of dopamine in the previous figure (Figure 4.2) shows well electron transfer, which is quasi-reversible, while the irreversible cyclic voltammogram was obtained from ascorbic acid. The quasi-reversible voltammogram of dopamine means that reduction currents can be observed even though they are lower than oxidation currents. In addition, cathodic potentials can be applied for

measurement of DA, which could be beneficial due to less interferences. For irreversible voltammogram of ascorbic acid, only oxidation currents can be measured and anodic potentials can be used.

From previous results, two advantages of the chip bonded using ethanol (reversible bonding) were found. First, the reversible bonding chip gives better sensitivity for detection with higher current approximately 50 times compared with the current obtained from the plasma bonding device. Second, the reversible bonding chip has a wider potential range than the plasma-bonding one.

4.2 Droplet with Electrochemical Detection

Water-in-oil droplets were generated using a T-junction microfluidic device. This device consists of main channels (100 μm deep, 500 μm wide) and a narrow channel (100 μm deep, 50 μm wide and 5 mm long) at the detection area where microband electrodes were placed across the narrow channel, as seen in Figure 1.5. To generate droplets, an oil solution was pumped at a flow rate of 1.8 $\mu\text{L}/\text{min}$ whereas a flow of 0.8 $\mu\text{L}/\text{min}$ was applied to an aqueous inlet. Droplets travelling along the main channel were squeezed through the narrow channel and passed the electrodes at which the droplet contents were monitored for chronoamperometric detection. To find a suitable potential, a hydrodynamic voltammogram was generated. In addition, effects of water fraction and total flow rate on chronoamperometric measurements were studied and optimized.

4.2.1 Hydrodynamic voltammogram

Currents from chronoamperometric measurements of DA and AA were plotted as a function of the applied potential, as shown in Figure 4.3. After that, graphs of hydrodynamic voltammograms were created by plotting current signal to noise (S/N) ratio obtained from the graphs in Figure 4.3 versus applied potential. Hydrodynamic voltammograms of 0.1 mM DA and AA are presented in Figure 4.4.

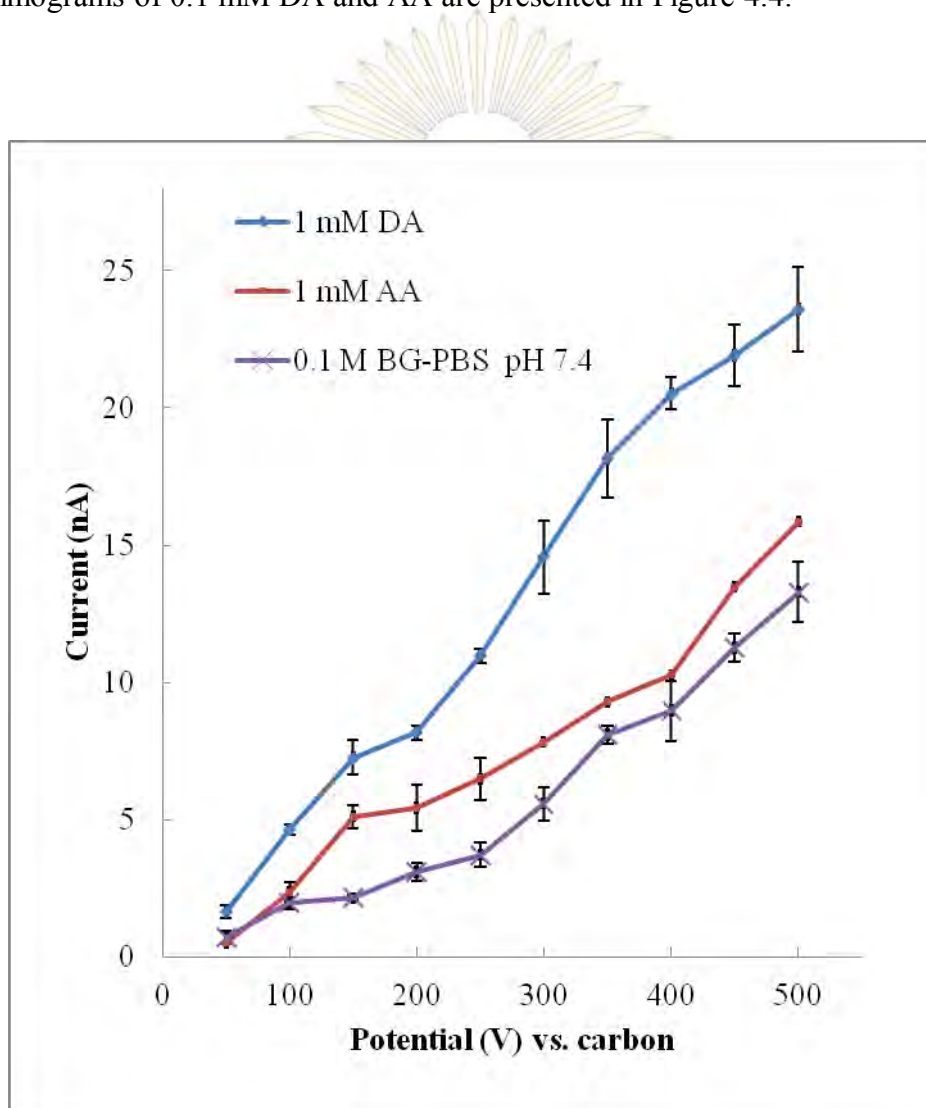


Figure 4.3 Chronoamperometric currents of dopamine, ascorbic acid and background electrolyte at different applied potentials. Droplet were generated using total flow rate of 2.6 $\mu\text{L}/\text{min}$ (0.016 mm/s) and $W_f = 0.31$.

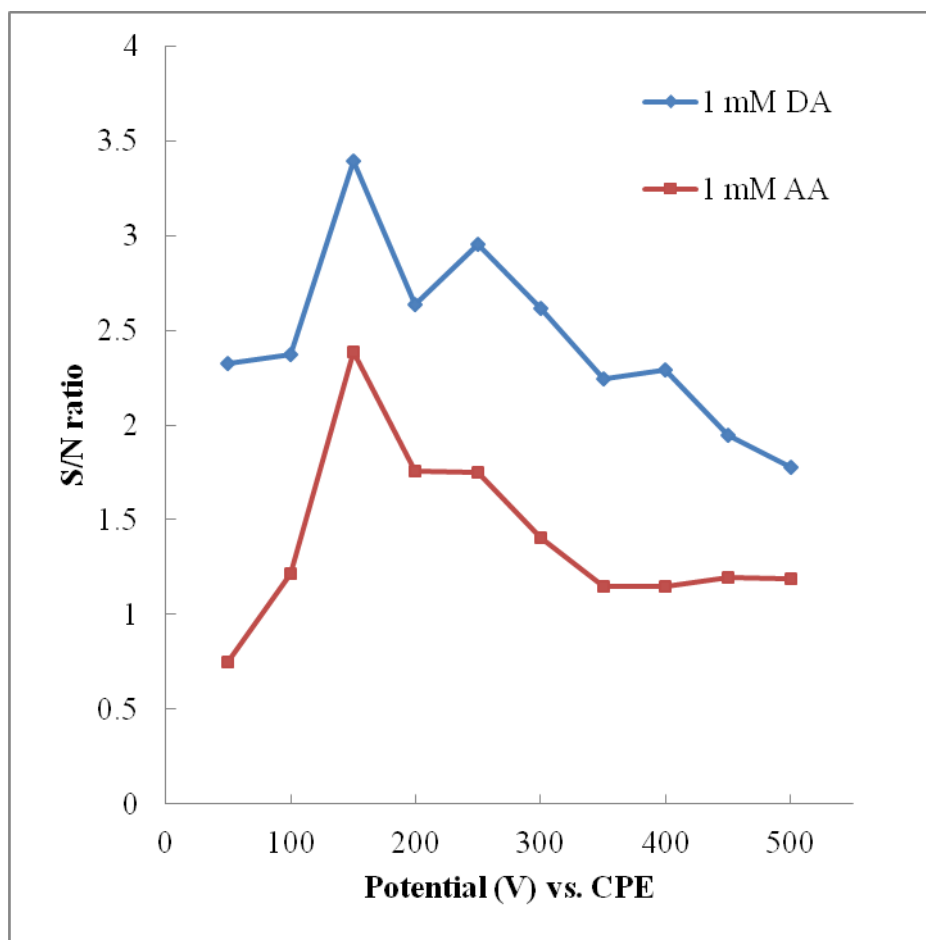


Figure 4.4 Hydrodynamic voltammograms of dopamine and ascorbic acid. Conditions for droplet generation is shown in Figure 4.3.

From Figure 4.4, an applied potential of 150 mV showed the highest S/N for both dopamine and ascorbic acid. In addition, S/N values of dopamine at any applied potential were higher than those of ascorbic acid. Therefore, 150 mV was an optimized potential for amperometric measurements of DA and AA using this system.

4.2.2 Chronoamperometry in droplets

Here, chronoamperometric measurements were performed in the droplet system. Droplets were generated using either 2 mM DA or 2 mM AA. The oil phase was delivered at a flow rate of $1.8 \mu\text{L}/\text{min}$ while the aqueous solution was pumped at a flow rate of $0.8 \mu\text{L}/\text{min}$. Chronoamperograms of 2 mM DA and AA obtained from the droplet system are shown in Figures 4.5 (a) and 4.5 (b). One peak represents to a droplet. As seen in figure 4.5, the initial current was high and decreased exponentially with time. The current was measured at the end of the droplet peak.

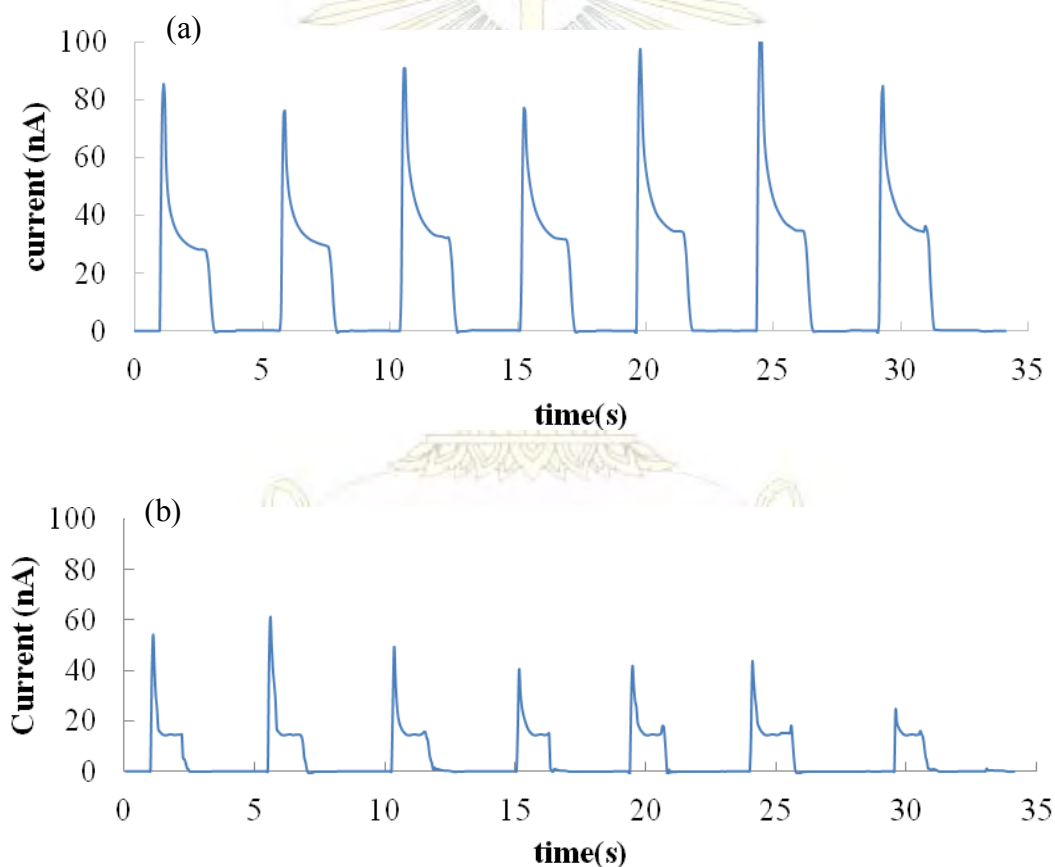


Figure 4.5 Chronoamperometric readouts of 35-s window for droplets containing 2 mM DA (a) and AA (b) in 0.1 M PBS pH 7.4. This experiment was carried out using a total flow rate of $2.6 \mu\text{L}/\text{min}$ ($0.016 \text{ mm}/\text{s}$) and $W_f = 0.31$. The applied potential was 150 mV.

The amperograms above show that dopamine gave higher currents than ascorbic acid does at the same applied potential, which agreed with the hydrodynamic voltammogram results. The currents were measured at the end of the peaks. The measured current is not only dependent on analysis time while a droplet passed through the electrodes, but it also relies on concentration of the analyte. The longer analysis times mean that more signals can be collected. The measured currents were ~22 and ~15 nA for DA and AA, respectively.

4.2.3 Effect of water fraction on chronoamperometric detection

Drop size or water fraction (W_f) must be optimized for best results of amperometric detection. Water fraction (calculated using Equation 2.2) is related to flow rates of aqueous and oil solutions. The higher the water fraction, the longer the droplet size, due to more aqueous coming through the droplets. To study effect of W_f on amperometric currents, total flow rate was fixed at 2.6 $\mu\text{L}/\text{min}$ and W_f was varied in the range of 0.15 to 0.46. Currents obtained from each W_f are shown in Table 4.1.

Table 4.1 Effect of water fraction on chronoamperometric measurements of 1 mM dopamine when using total flow rate of 2.6 $\mu\text{L}/\text{min}$ and a 150 mV applied potential.

Oil ($\mu\text{L}/\text{min}$)	Aqueous ($\mu\text{L}/\text{min}$)	Total ($\mu\text{L}/\text{min}$)	water fraction (W_f)	Current (nA)
1.4	1.2	2.6	0.46	3.78
1.6	1.0	2.6	0.38	4.40
1.8	0.8	2.6	0.31	10.1
2.0	0.6	2.6	0.23	8.56
2.2	0.4	2.6	0.15	7.92

A graph representing currents measured from each water fraction is shown in Figure 4.6. The best water fraction for this system is 0.31 because it gave the highest chronoamperometric current of ~ 10 nA. Lower water fractions than 0.31 showed slightly lower currents. This could be because the analysis time is not long enough for electrochemical detection due to smaller droplet sizes. For higher water fractions than 0.31, the droplets were too long for chronoamperometric measurements. This resulted in low measured currents because the currents almost reached the background. This is due to the fact that chronoamperometric currents decrease exponentially with time. It should be noted that in this experiment, currents were measured at the end of the droplet peaks, so larger droplets resulted in lower measured currents.

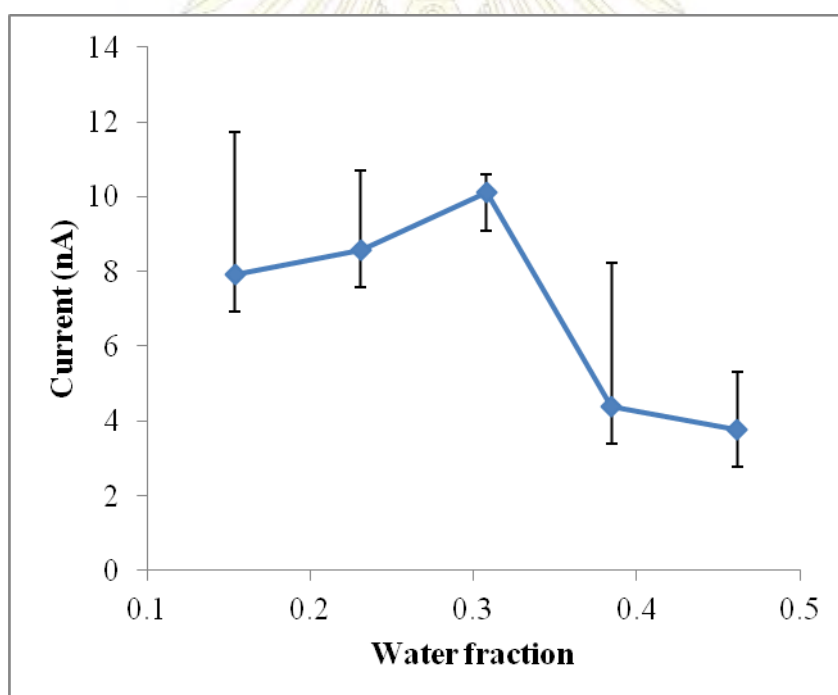


Figure 4.6 Effect of W_f on amperometric measurements. Droplets were generated using 1 mM DA with total flow rate of $2.6 \mu\text{L}/\text{min}$ and the applied potential was 150 mV.

4.2.4 Effect of total flow rate on chronoamperometric detection

Total flow rate in the system is the summation of flow rates of all inlets of the microdevice. Total flow rate is really important in this work because electrochemistry requires longer analysis time than optical detection for droplets to be detected. The water fraction was fixed when varying the total flow rate in this system. Effect of the total flow rate on chronoamperometric measurements is presented in Table 4.2 and Figure 4.7.

Table 4.2 Effect of total flow rate on amperometric measurements of 1 mM DA when using $W_f = 0.31$ and a 150 mV applied potential.

Oil ($\mu\text{L}/\text{min}$)	Aqueous ($\mu\text{L}/\text{min}$)	Total ($\mu\text{L}/\text{min}$)	Water fraction (W_f)	Current (nA)
0.90	0.40	1.30	0.31	1.42
1.35	0.60	1.95	0.31	10.4
1.80	0.80	2.60	0.31	10.0
2.25	1.00	3.25	0.31	N/A
2.70	1.20	3.90	0.31	N/A

*N/A is undetectable.

ภาควิชาเคมี
คณะวิทยาศาสตร์
จุฬาลงกรณ์มหาวิทยาลัย

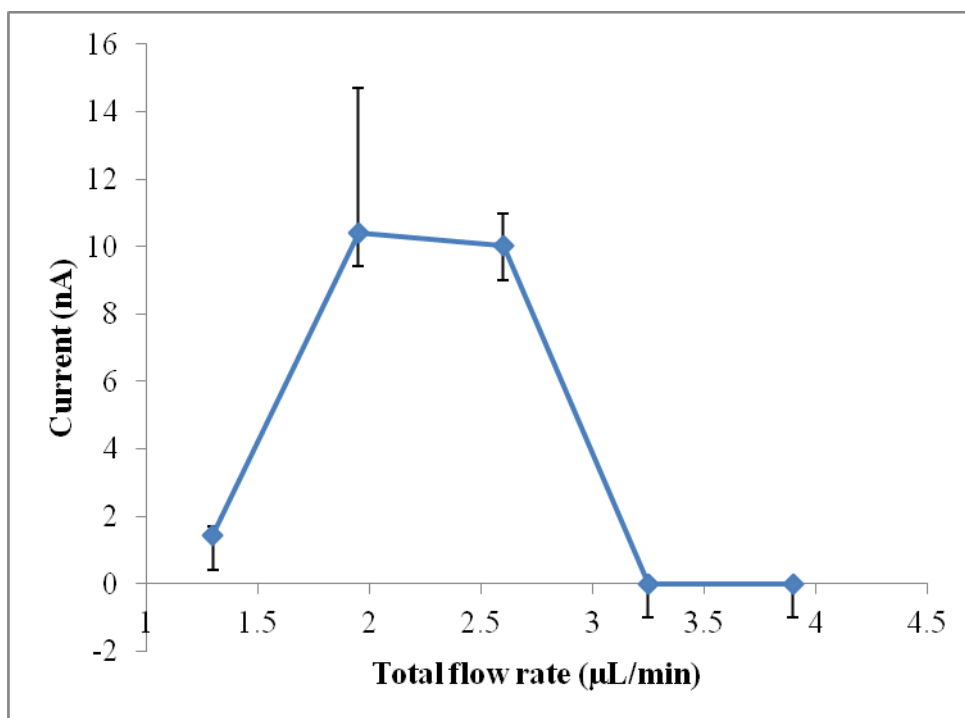


Figure 4.7 Effect of total flow rate on amperometric measurements. Droplets were generated using 1 mM DA with $W_f = 0.31$ and a 150 mV applied potential.

Although the total flow rate of 1.95 $\mu\text{L}/\text{min}$ gave the highest current in the experiment, using low flow rates can cause unstable droplet formation. Moreover, the flow rate at 2.6 $\mu\text{L}/\text{min}$ gave no significant difference in chronoamperometric current when compared to the flow rate at 1.95 $\mu\text{L}/\text{min}$. Furthermore, this flow rate also could be better for high-throughput analysis. Therefore, a total flow rate at 2.6 $\mu\text{L}/\text{min}$ was chosen. At higher flow rates, currents could not be measured, because the analysis time was not enough for electrochemical detection. In addition, the lower flow rate showed low measured currents, because low flow rates resulted in long analysis time, which could give the chronoamperometric current decreased exponentially with time. So, the longer analysis time, the lower the measured current.

Therefore, the optimum conditions of this system depends on an applied potential, water fraction and total flow rate. The optimum applied potential in this work is 150 mV and the water total flow rate and water fraction in this work are 2.6 $\mu\text{L}/\text{min}$ and 0.31, respectively. These optimized parameters were used for quantitative measurements of dopamine and ascorbic acid.

4.3 Method of Validation

4.3.1 Calibration curve

Calibration curves of dopamine and ascorbic acid were created from results obtained from chronoamperometric detection in the droplet-based microfluidic system. A concentration series of DA and AA was prepared at 0.5, 1, 1.5, 2 and 2.5 mM in 0.1 M PBS (pH 7.4). Chronoamperometric measurements were performed for 1 minute for each concentration. Figures 4.8 (a) and 4.8 (b) are overlay chronoamperograms of a single droplet with different concentrations of DA and AA. Figures 4.9 (a) and (b) show examples of detected droplets containing different concentrations of DA and AA.



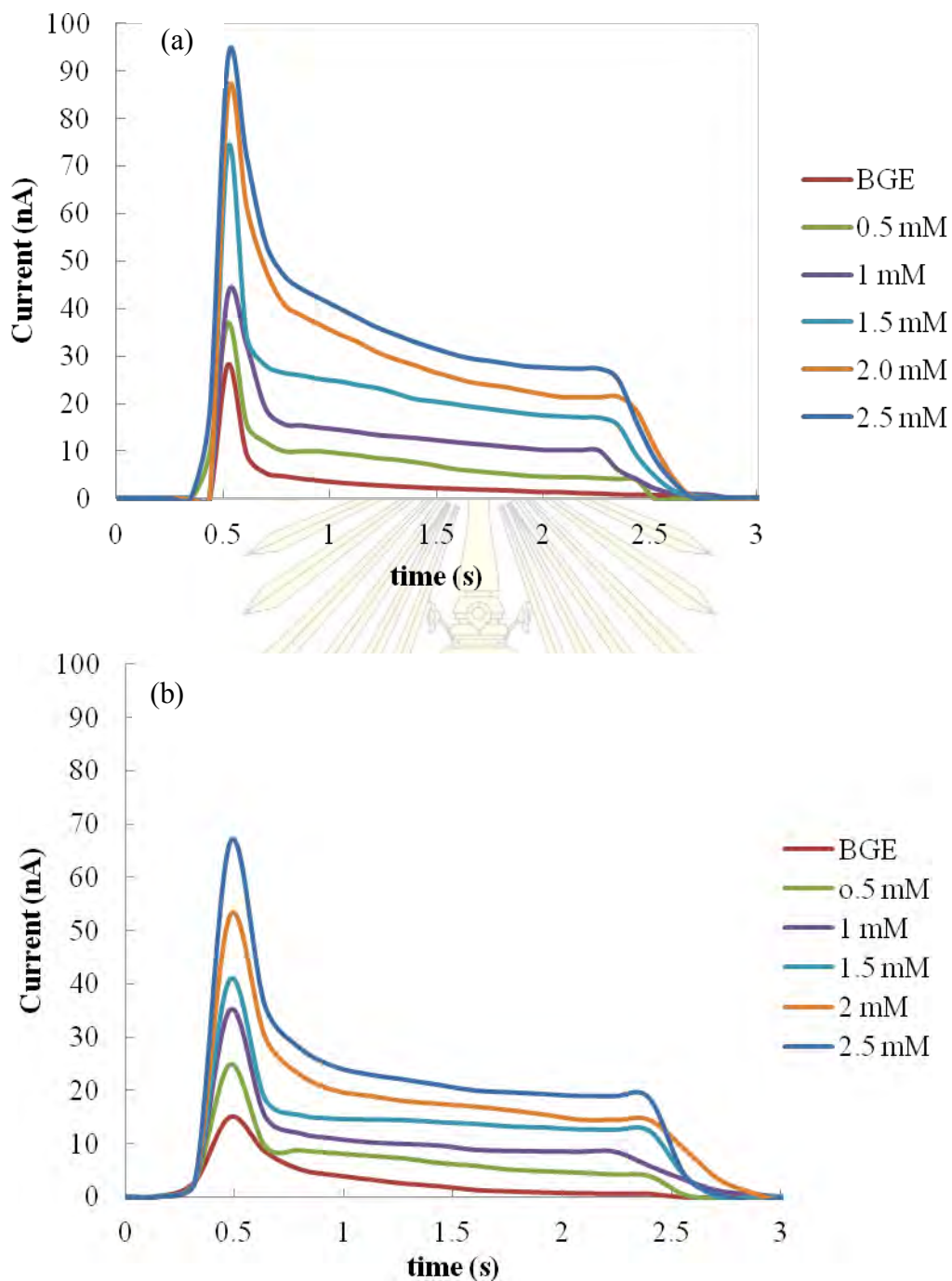


Figure 4.8 Chronoamperometric signals obtained from a single droplet containing different (a) DA and (b) AA concentrations. Droplets were generated using total flow rate of $2.6 \mu\text{L}/\text{min}$ and $W_f = 0.31$. The applied potential was 150 mV.

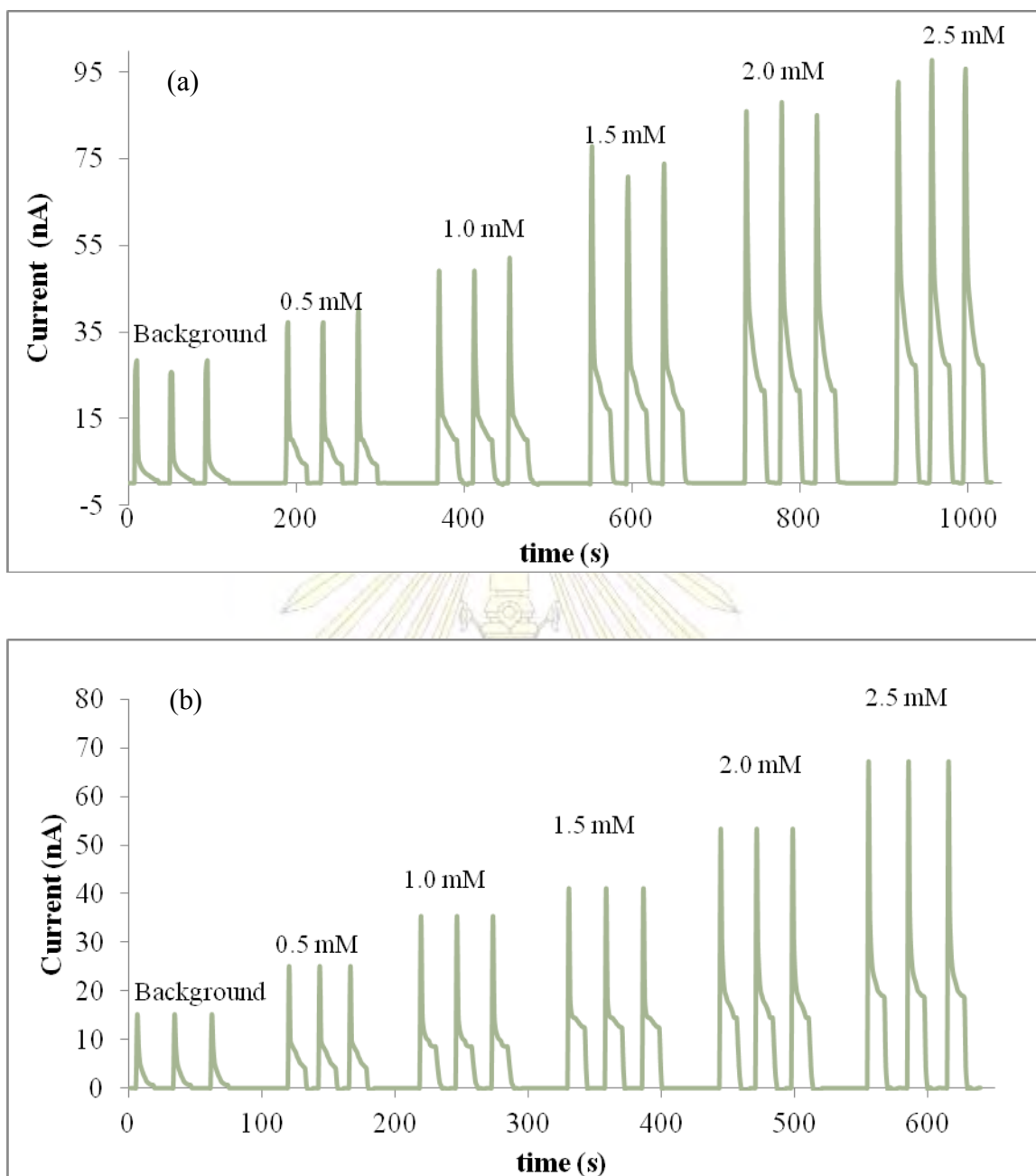


Figure 4.9 Chronoamperograms of (a) DA and (b) AA at different concentrations measured from the droplet system.

As seen in Figure 4.9, each DA concentration gave different currents which are 4.71, 10.4, 17.3, 22.3, and 27.5 nA for 0.5, 1, 1.5, 2 and 2.5 mM, respectively. The higher the concentration, the higher the current. AA also gave the same trend of results.

After that, the concentration series of DA and AA were plotted versus averaged currents to construct calibration curves in Figures 4.10 (a) and 4.10 (b).

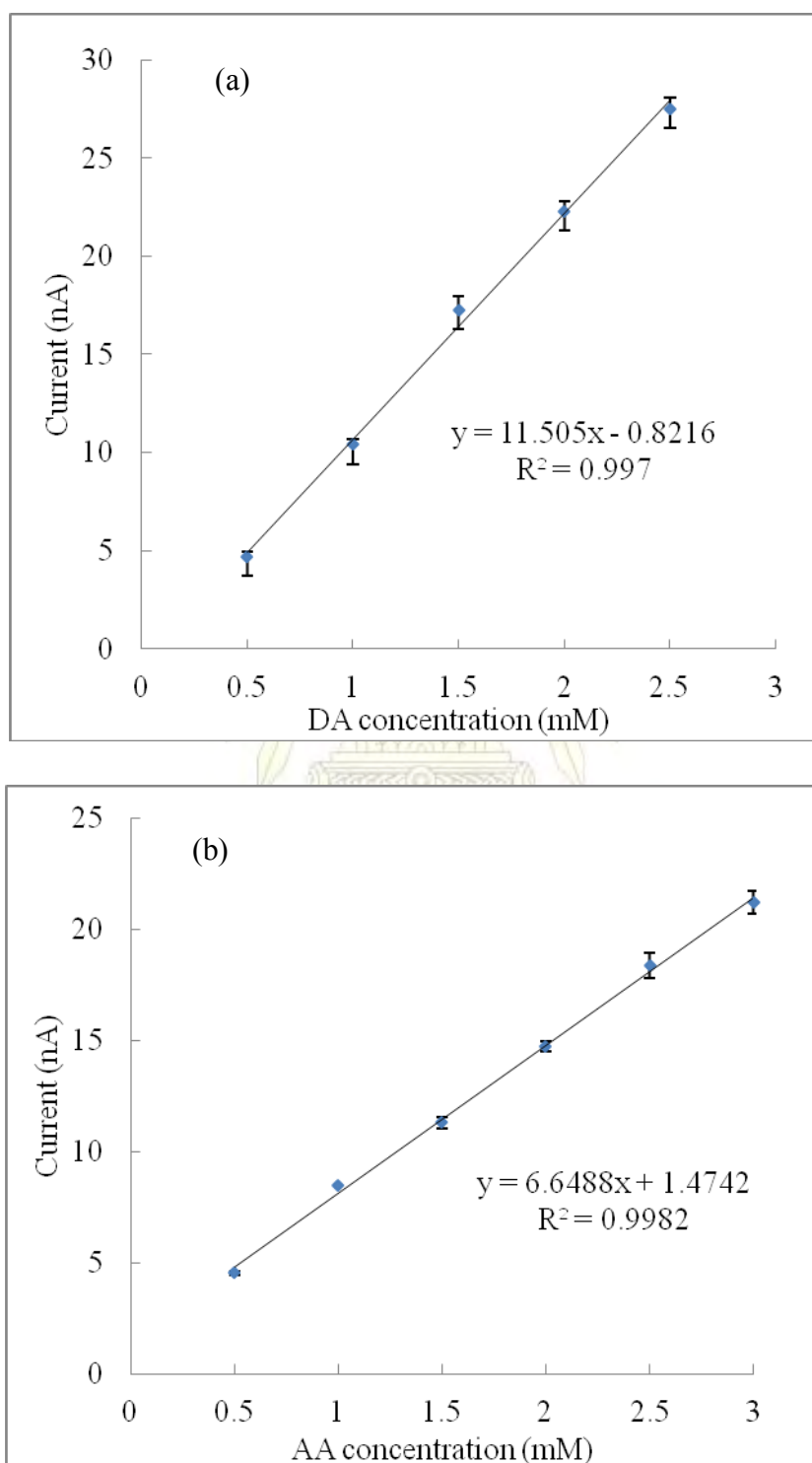


Figure 4.10 Calibration curves of (a) DA and (b) AA. Conditions for droplet formation and the applied potential were the same as in Figure 4.8.

A good linear relationship was obtained for DA and AA calibration plots with R^2 values equal to 0.9970 and 0.9982, respectively.

4.3.2 **Limit of detection (LOD) and limit of quantitation (LOQ)**

For this system, LOD and LOQ were 20 μM ($S/N = 3$) and 70 μM ($S/N = 10$) for DA. Furthermore, LOD and LOQ of AA were found to be 41 and 137 μM , respectively.

4.3.3 **Linearity**

The calibration curves of analytes were created using the results obtained from chronoamperometry. Although linear equations and R^2 values were obtained, a linear range is not yet reported. So, higher and lower concentrations of DA and AA than the concentration range used in the calibration curves were prepared. Higher concentrations were prepared at 3, 5 and 8 mM in 0.1 M PBS. Lower concentrations were prepared at 0.08 and 0.02 mM for DA, and 0.04 and 0.14 mM for AA. The DA concentration at 0.02 mM (20 μM) was prepared for LOD rechecking. Another concentration of 0.08 mM (80 μM) was prepared because it is a normal DA concentration in human serum.

Here, LOD was rechecked and found that the LOD from the experiment agreed with that from the calculation. Linearity of DA solution in this system was reported in a range of 0.02-3.0 mM, as shown in Figure 4.11 (a). In addition, linearity of AA was reported in a range of 0.04-3.0 mM, as shown in Figure 4.11 (b). The higher concentrations (>3 mM) were out of the line because of small working area of the microelectrodes. This could limit the amount of analytes to be detected.

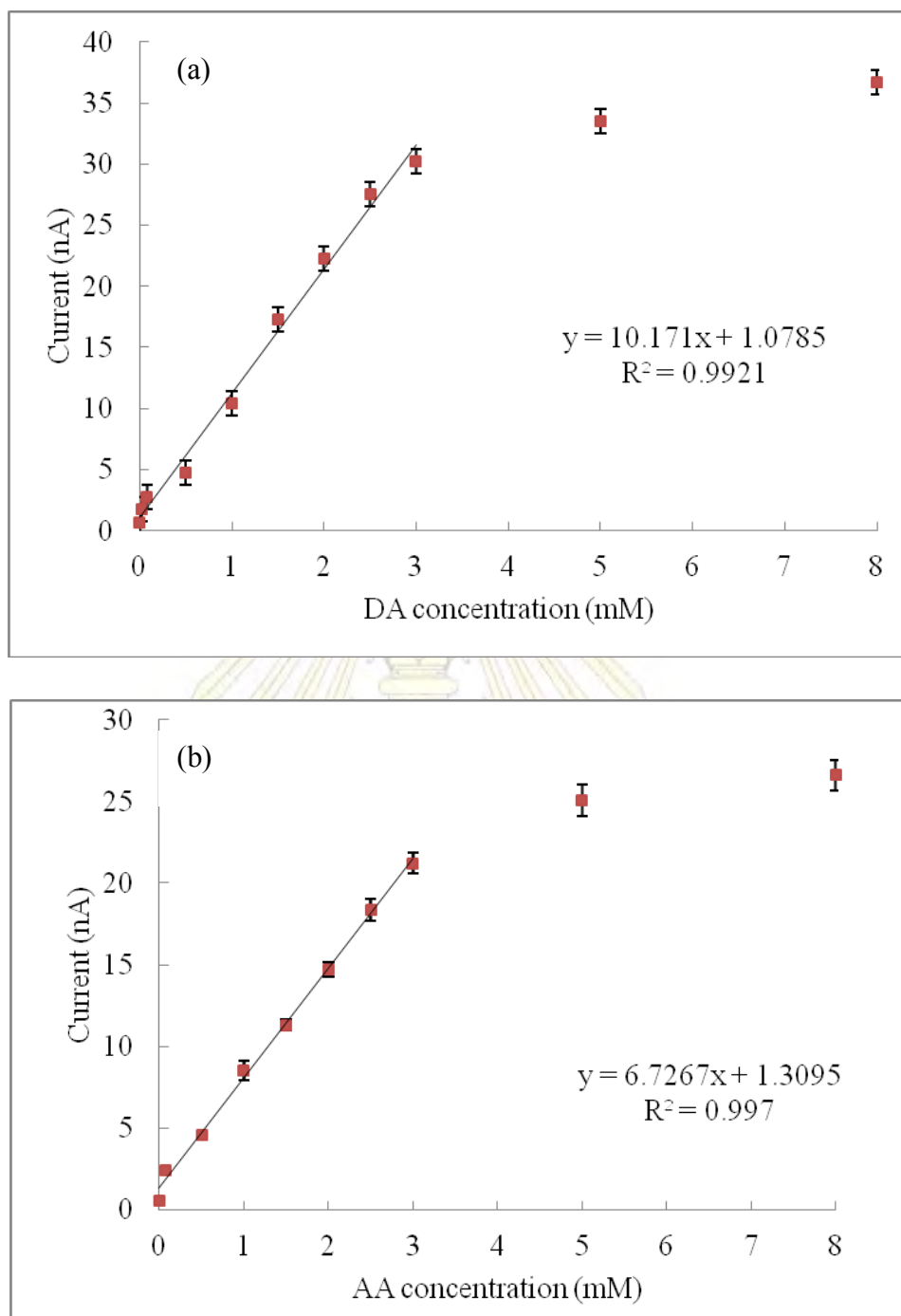


Figure 4.11 The linear range of current signals obtained from the droplet system with electrochemical detection when measuring DA (a) and AA (b) at different concentrations. Other conditions for droplet generation and the applied potential are shown in Figure 4.8.

4.3.4 Precision

Inter-day and intraday measurements of droplets containing an analyte were reported to determine precision of the droplet system for DA and AA analysis in this work. An inter-day experiment was carried out for days ($n = 3$) in a week by measuring 1.5 mM DA and AA solutions. The percentage of relative standard deviation (%RSD) was used to evaluate repeatability of this method. Table 4.3 shows inter-day precision of measurements of DA and AA using the droplet system. High inter-day precision was obtained for measurements of DA & AA with %RSD less than 3%.

Table 4.3 Inter-day measurements of DA and AA, the experiments were carried out in 3 days ($n = 3$).

Day	Averaged Current (nA)	
	DA	AA
1	17.71	12.59
2	17.26	12.59
3	17.75	11.98
Average	17.57	12.39
SD	0.24	0.32
%RSD	1.38	2.54

For intraday precision, 0.5, 1.5 and 2.5 mM DA and AA were used. The currents were measured using 50 droplets for each concentration. Figure 4.12 shows graphs of currents measured from 50 droplets for each concentration of DA and AA. The graphs show that there are slight variation in the measured currents, indicating high precision of the system for measurements of DA and AA. The averaged currents obtained from this method were 4.73, 17.35 and 27.53 nA for 0.5, 1.5 and 2.5 mM DA, and 4.71, 12.04 and 18.24 nA for 0.5, 1.5 and 2.5 mM AA, respectively (Figure 4.12 and Table 4.4). The values of %RSD of this evaluation were reported in the ranges of 3.25-4.70% for DA and 2.84 – 4.98% for AA.

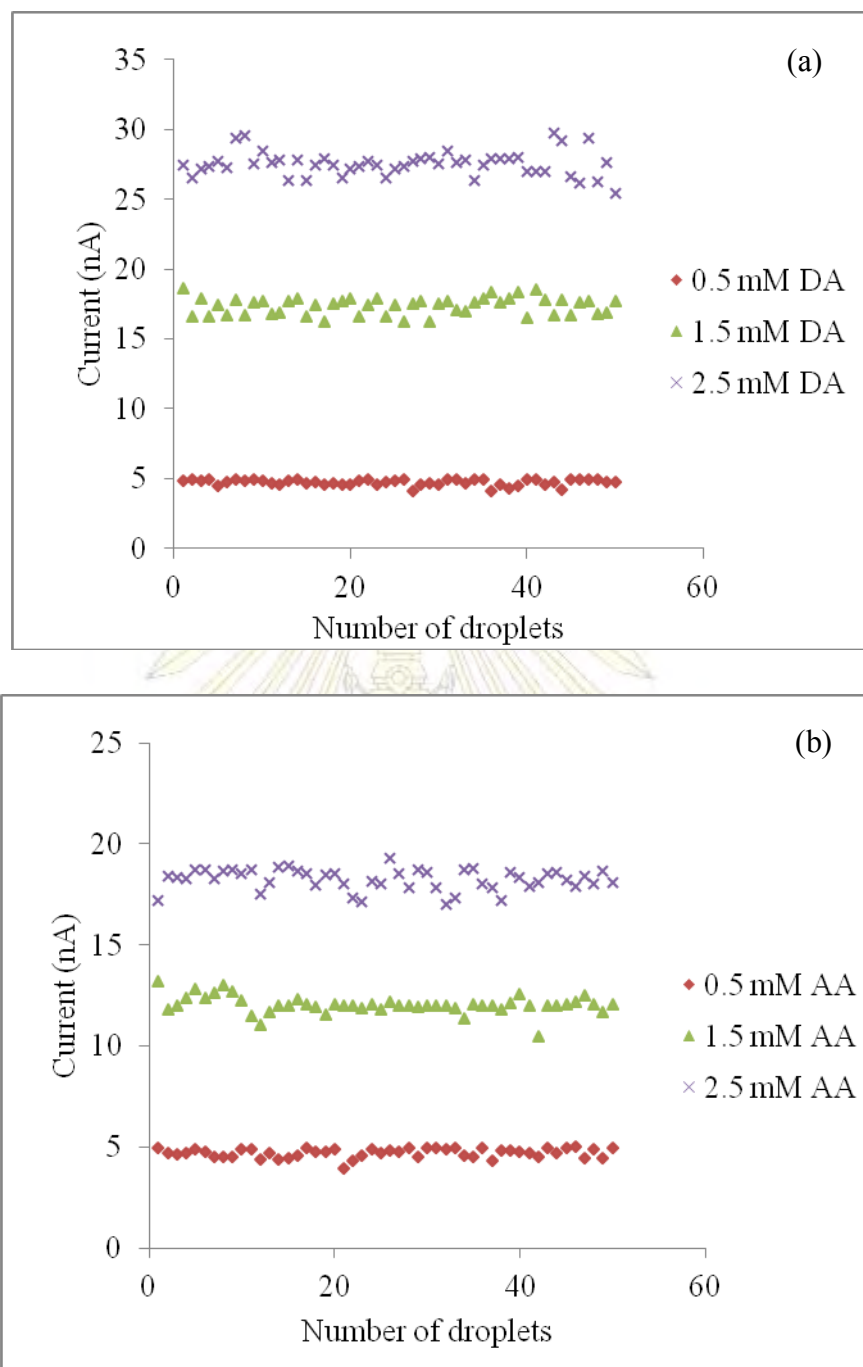


Figure 4.12 Amperometric currents obtained from measurements of 50 droplets containing 0.5, 1.5 and 2.5 mM DA (a) and AA (b). Each concentration was separately measured.

Table 4.4 Intraday precision of DA and AA measurements. The currents were averaged from 50 droplets ($n = 50$) for each concentration.

Concentration (mM)	Averaged current (nA)		%RSD	
	DA	AA	DA	AA
0.5	4.73±0.22	4.71±0.23	4.70	4.98
1.5	17.35±0.62	12.04±0.43	3.60	3.59
2.5	27.53±0.90	18.24±0.52	3.25	2.84

From Table 4.4, the averaged values of the currents from each concentration give %RSD less than 5%, indicating high intraday precision of the method.

4.4 Real Sample Measurements

Three commercial brands of DA injection were measured. All DA solutions were diluted to be a concentration of 1 mM before measurements. Chronoamperometric currents of each DA sample obtained from the measurements were calculated to be concentrations using the calibration curve in Figure 4.10 (a). An AA sample solution was prepared at a concentration of 1.5 mM and measured using the droplet system. Chronoamperometric currents of the AA sample obtained from the measurements were calculated to be concentrations using the calibration curve in Figure 4.10 (b).

Results obtained from the real sample measurements are shown in Table 4.5. The concentrations of DA in the 3 samples were found to be 242.5, 245.0 and 188 mg/10 mL for UPAMINE, DOPAMINE and DOPAMEX, respectively. The measured amounts were slightly lower than the labeled concentrations. The negative errors for DA measurements are -1.8, -2.6 and -5.7%, which are not significantly different from the labeling. For AA, the measured amount was reported to be 510 mg/2 mL, which gives a positive error of 1.8%.

The negative errors of DA concentration in the real samples could come from the stabilizer (that may be a citric buffer) in medical products. Citric buffer and other components could interfere the electrochemical oxidation process of DA. Furthermore, it could be due to human errors in sample preparation steps. The positive error of ascorbic acid in the real sample could come from the other components that may be electroactive species which can also give current signals.

Table 4.5 The concentrations of DA and AA in real samples which are measured using the droplet system.

Brand	Content	The measured concentration (mM)	The labeled amount	The measured amount	%RSD	%Error
UPAMINE (1mM)	Dopamine	0.97±0.03	250 (mg/ 10 mL)	242.5 (mg/ 10 mL)	3.02	-2.6
DOMINE (1mM)		0.98±0.03	250 (mg/ 10 mL)	245 (mg/ 10 mL)	3.33	-1.8
DOPAME X (1 mM)		0.94±0.02	200 (mg/ 10 mL)	188 (mg/ 10 mL)	2.66	-5.7
Vitamin C (1.5 mM)	Ascorbic acid	1.53±0.03	500 (mg/ 2 mL)	510 (mg/ 2 mL)	2.43	1.8

Chapter 5

Conclusions

Here, an application of droplet-based microfluidics coupled with an electrochemical sensor using chronoamperometry with chip-based carbon paste electrodes (CPEs) for determination of dopamine (DA) and ascorbic acid (AA) was reported. A microchip having a narrow channel across three band CPEs was used to elongate droplets for longer analysis time of electrochemical measurements. A reversible ethanol bonding was used for device assembly in this work for improving sensitivity of CPEs and preventing the decomposition of noujol oil from oxygen plasma treatment.

For chronoamperometric measurements of DA and AA using this approach, droplets were generated using either DA or AA solutions at a flow rate of 0.8 $\mu\text{L}/\text{min}$. The oil flow rate was 1.8 $\mu\text{L}/\text{min}$, resulting a water fraction of 0.31. The optimum potential was 150 mV. Highly reproducible analysis of DA and AA was achieved with relative standard deviations (%RSD) less than 5% for both intraday and inter-day measurements. Limit of detection (LOD) and limit of quantitation (LOQ) were found to be 20 and 70 μM for DA and 41 and 137 μM for AA. The dynamic ranges of this method were in the ranges of 0.02-3.0 mM for DA and 0.04-3.0 mM for AA. This system was successfully applied to determine the amount of DA and AA in intravenous drugs. Calibration curves of DA and AA for quantitative analysis were obtained with good linearity with R^2 values of 0.9970 and 0.9982, respectively. Compared with the labeled amounts, the measured concentrations of DA and AA obtained from the droplet system were slightly different with the error percentages of +1.8% for AA and in the range of -2.6 to -5.7% for DA, indicating high accuracy of the method. From this work, the droplet system is not only useful for measurements of

drug contents, but this approach would make a great promise for applications in analysis of cells and microorganisms. In addition, the portability of the method would be beneficial for real field analysis.



REFERENCES

1. Whitesides, G.M. The origins and the future of microfluidics. *Nature* **2006**, *442*, 368-373.
2. Thorsen, T.; Roberts, R.W.; Arnold, F.H.; Quake, S.R. Dynamic pattern formation in a vesicle-generating microfluidic device. *Phys. Rev. Lett.* **2001**, *86*, 4163-4166.
3. Song, H.; Tice, J.D.; Ismagilov, R.F. A microfluidic system for controlling reaction networks in time. *Angew. Chem. Int. Ed.* **2003**, *42*, 767-772.
4. Zhu, Y.; Fang, Q. Analytical detection techniques for droplet microfluidics-a review. *Anal. Chim. Acta.* **2013**, *787*, 24-35.
5. Kovarik, M.; Ornoff, D.; Melvin, A.; Dobes, N.; Wang, Y.; Dickinson, A.; Gach, P.; Shah, P.; Allbritton, N. Micro total analysis systems: fundamental advances and application in the laboratory, clinic, and field. *Anal. Chem.* **2013**, *85*, 451-472.
6. Huebner, A.; Srisa-Art, M.; Holt, D.; Abell, C.; Hollfelder, F.; deMello, A.J.; Edel, J. B. Quantitative detection of protein expression in single cells using droplet microfluidics. *Chem. Commun.* **2007**, 1218-1220.
7. Bai, Y.; He, X.; Liu, D.; Patil, S.N.; Bratton, D.; Huebner, A.; Hollfelder, F.; Abell, C.; Huck, W.T.S. A double droplet traps system for studying mass transport across a droplet-droplet interface. *Lab Chip* **2010**, *10*, 1281-1285.
8. Ji, J.; Zhao, Y.; Guo, L.; Liu, B.; Ji, C.; Yang, P. Interfacial organic synthesis in a simple droplet-based microfluidic system. *Lab Chip* **2012**, *12*, 1373-1377.
9. Lazarus, L.; Riche, T.C.; Marin, B.C.; Gupta, M.; Malmstadt, N.; Brutchey, R.L. Two-phase microfluidic droplet flows of ionic liquids for the synthesis of gold and silver nanoparticles. *Appl. Mater. Interfaces* **2012**, *4*, 3077-3083.
10. Mary, P.; Studer, V.; Tabeling, P. Microfluidic droplet-based liquid-liquid extraction. *Anal. Chem.* **2008**, *80*, 2680-2687.

11. Chang, C.; Sustarich, J.; Bharadwaj, R.; Chandrasekaran, A.; Adamsand, P.D.; Singh, A.K. Droplet-based microfluidic platform for heterogeneous enzymatic assays. *Lab Chip* **2013**, *13*, 1817-1822.
12. Guo, M.T.; Rotem, A.; Heymanand, J.A.; Weitz, D.A. Droplet microfluidics for high-throughput biological assays. *Lab Chip* **2012**, *12*, 2146-2155.
13. Goh, L.; Chen, K.; Bhamidi, V.; He, G.; Kee, N.C.S.; Kenis, P.J.A., Zukoski, C.F., III.; Braatz, R.D. A stochastic model for nucleation kinetics determination in droplet-Based microfluidic systems. *Cryst. Growth Des.* **2010**, *10*, 2515–2521.
14. Lui, H.; Crooks, R.M. Highly reproducible chronoamperometric analysis in microdroplets. *Lab Chip* **2013**, *13*, 1364.
15. Moehlenbrock, M; Martin, R.S. Development of an on-chip injector for microchip-based flow analyses using laminar flow. *Lab Chip* **2007**, *7*, 1589-1796.
16. Wang, J.; Polsky, R.; Tian, B.; Chatrathi M.P. Voltammetry on microfluidic chip platforms. *Anal. Chem.* **2000**, *72*, 5285-5289.
17. Zoe, Z.; Jang, A.; MacKnight, E.; Wu, P.; Do, J.; Bishop, P.L.; Ahn, C.H. Environmentally friendly disposable sensors with microfabricated on-chip planar bismuth electrode for *in situ* heavy metal ions measurement. *Sens. Actuat. B. chem.* **2008**, *134*, 18-24.
18. Jothimuthu, P.; Wilson, R.A.; Herren, J.; Haynes, E.N.; Heineman, W. R.; Papautsky, I. Lab-on-a-chip sensor for detection of highly electronegative heavy metals by anodic stripping voltammetry. *Biomed. Microdevices* **2011**, *13*, 695–703.
19. Silva, R.; Almeida, E.; Rabelo, A.; Silva A.; Ferreira, L.; Richter, E. Three electrode electrochemical microfluidic cell: construction and characterization. *J. Braz. Chem. Soc.* **2009**, *20*, 1235-1241.
20. Lou, C.; Yang, X.; Fu, Q.; Sun, M.; Ouyany, Q.; Chen, Y.; Ji, H. Picoliter-volume aqueous droplets in oil: Electrochemical detection and yeast cell electroporation. *Electrophoresis* **2006**, *27*, 1977-1983.

21. Lui, S.; Gu, Y.; Roux, R.B.L.; Matthews, S.M.; Bratton, D.; Yunus, K.; Fisher, A.C.; Huck, W.T.S. The electrochemical detection of droplets in microfluidic devices. *Lab Chip* **2008**, *8*, 1937-1942.
22. Han, Z.; Li, W.; Huang, Y.; Zheng, B. Measuring rapid enzymatic kinetics by electrochemical method in droplet-based microfluidic devices with pneumatic valves. *Anal. Chem.* **2009**, *81*, 5840-5845.
23. Itoh, D.; Sassa, F.; Nishi, T.; Kani, Y.; Murata, M.; Suzuki, H. Droplet-based microfluidic sensing system for rapid fish freshness determination. *Sens. Actuat. chem. B.* **2012**, *171-172*, 619-626.
24. Sameenoi, Y.; Mensack, M.; Boonsong, K.; Ewing, R.; Dungchai, W.; Chailapakul, O.; Cropek, D.M.; Henry, C.S. Poly(dimethylsiloxane) cross linked carbon paste electrodes for microfluidic electrochemical sensing. *Analyst* **2011**, *136*, 3177-3184.
25. Sameenoi Y.; Koehler K.; Shapiro, J.; Boonsong, K.; Sun, Y.; Collett, J. Jr.; Volckens, J.; Henry, C.S. Microfluidic electrochemical sensor for on-line monitoring of aerosol oxidative activity. *J. Am. Chem. Soc.* **2012**, *134*, 10562-10568.
26. Srisa-Art, M. Microdroplet reactors for high-throughput chemistry and biology. Ph.D. Thesis, Imperial College London, **2010**.
27. Wu, L.; Xu, W.; Bachman, M.G.P. Passive generation of droplets in mini and microchannels. ASME 5th International Conference on Nanochannels, Microchannels, and Minichannels, Puebla, Mexico, June 18–20, 2007.
28. Tice, J.D.; Song, H.; Lyon, A.D.; Ismagilov, R.F. Formation of droplets and mixing in multiphase microfluidics at low values of the reynolds and the capillary numbers. *Langmuir* **2003**, *19*, 9127-9133.
29. Song, H.; Chen, D.L.; Ismagilov, R.F. Reactions in droplets in microfluidic channels. *Angew. Chem. Int. Ed.* **2006**, *45*, 7336 – 7356.
30. deMello, A.J. Control and detection of chemical reactions in microfluidic systems. *Nature* **2006**, *442*, 394-402.
31. Bringer, M.R.; Gerdts, C.J.; Song, H.; Tice, J.D.; Ismagilov, R.F. Microfluidic systems for chemical kinetics that rely on chaotic mixing in droplets. *Phil.Trans. R. Soc .Lond. A.* **2004**, *362*, 1087-1104.

32. Duffy, D.C.; McDonald, J.C.; Schueller, O.J.A.; Whitesides, G.M. Rapid prototyping of microfluidic systems in poly(dimethylsiloxane). *Anal. Chem.* **1998**, *70*, 4974-4984.
33. Bard, A.J.; Faulkner, L.R. *Electrochemical methods: Fundamentals and Applications*, 2nd ed.; John Wiley & Sons, Inc.: New York, **2001**.
34. Skoog, D.A.; Holler, F.J.; Crouch, S. R. *Principles of Instrumental Analysis*, 6th ed.; Brooks/Cole, Cengage Learning: California, **2007**.
35. Instruction manual for basi epsolon for electrochemistry home page.<http://www.basinc.com> (21 February 2014).
36. Kelloner, R.; Mermet, J.M.; Otto, M.; Valcarcel, M.; Widmer, H.M. *Analytical Chemistry: A Modern Approach to Analytical Science*, 2nd ed; John Wiley & Sons, Inc.: New York, **2004**.



VITA

Mr.Akkpol Suea-ngam was born on Tuesday 8th October 1991 in Bangkok, Thailand. In 2010, he graduated a high school level from a Science division from Suankularb Wittayalai School, Bangkok, Thailand. After that, he studied for the Bachelor's degree of Science in Chemistry, Chulalongkorn University and complete in 2014. His address after graduation is 97 Phetkasem road, soi Phetkasem 53, Bangkae, Bangkok,Thailand.

